

Vanadium dioxide for thermochromic smart windows in ambient conditions



Nan Shen ^a, Shi Chen ^a, Runqing Huang ^a, Jiaqi Huang ^a, Jingyi Li ^a, Run Shi ^a, Shuzhang Niu ^a, Abbas Amini ^e, Chun Cheng ^{a,b,c,d,*}

^a Department of Materials Science and Engineering, Southern University of Science and Technology, Shenzhen, 518055, PR China

^b Key Laboratory of Energy Conversion and Storage Technologies (Southern University of Science and Technology), Ministry of Education, Shenzhen, 518055, China

^c Guangdong Provincial Key Laboratory of Energy Materials for Electric Power, Southern University of Science and Technology, Shenzhen, 518055, China

^d Shenzhen Engineering Research and Development Center for Flexible Solar Cells, Southern University of Science and Technology, Shenzhen, Guangdong Province, 518055, China

^e Center for Infrastructure Engineering, Western Sydney University, Kingswood, New South Wales, 2751, Australia

ARTICLE INFO

Article history:

Received 17 June 2021

Received in revised form

30 July 2021

Accepted 31 July 2021

Available online 8 August 2021

Keywords:

Doping

Electrothermal

Thermochromism

Integration

ABSTRACT

Smart windows have attracted increasing attentions in recent decades because of their ability to automatically regulate indoor solar irradiation, reduce the energy consumption of air-conditioning, and maintain comfortable thermal environment for indoors. As a typical thermochromic material, vanadium dioxide (VO_2) exhibits reversible metal-insulator transition accompanied with dramatic optical transmittance changes near the room temperature, which makes VO_2 -based smart windows promising for practical uses in ambient conditions. This review summarizes recent advancements of techniques utilized for tailoring the properties of VO_2 to meet the specific requirements for smart windows. The phase transition temperature (T_c) should be reduced approaching the room temperature, whereas luminous transmittance (T_{lum}) and solar energy modulation efficiency (ΔT_{sol}) must be high enough to capture adequate daylight and perform with an energy-saving trend. The doping strategy and integrating with functional coatings can regulate the properties of VO_2 films. Besides the passive response to ambient temperature, electrothermal techniques and integration with specific materials, which generate heat, can enable VO_2 to work with improved optical properties regardless of its higher T_c than the room temperature. Future maps for the development of VO_2 films are provided in the last part of the review.

© 2021 Elsevier Ltd. All rights reserved.

1. Introduction

Vanadium dioxide (VO_2) is a typical thermochromic (TC) material that undergoes a reversible metal-insulator transition (MIT) at a critical temperature (T_c) of 68 °C [1–3]. During this thermally induced MIT, VO_2 demonstrates a remarkable change of optical transmittance in the near-infrared spectral range [4,5], which represents its potential for energy-efficient smart windows (Fig. 1a). At temperatures less than T_c , VO_2 is transparent to near-infrared light with an insulating and monoclinic structure (Fig. 1b and c). VO_2 -based TC smart windows can pass near-infrared radiation and maintain desirable and comfortable environment in buildings. Above T_c , VO_2 presents a metallic rutile phase and is

opaque to near-infrared light (Fig. 1b and c), thus the near-infrared radiation can be blocked without raising the indoor temperature. Compared with other TC materials, VO_2 becomes more attractive owing to its negligible variation of luminous transmittance in response to temperature, which can offer adequate daylighting in buildings. These features of VO_2 make it an excellent candidate for the main component of modern smart windows.

VO_2 -based smart coatings have been extensively investigated for several decades [6,7], and yet many challenges exist before practical applications of smart windows [8]. To be specific, three shortcomings of VO_2 in TC properties exist, which include high T_c (68 °C), limited solar energy modulation ability (ΔT_{sol}), and low luminous light transmittance (T_{lum}). Many attempts, e.g. doping and integration techniques, have been made to modify the TC properties of VO_2 films, in particular approaching the T_c to the room temperature and enhancing T_{lum} and ΔT_{sol} values to higher levels.

* Corresponding author.

E-mail address: chengc@sustech.edu.cn (C. Cheng).

Moreover, the electrothermal strategy is used to induce MIT in VO_2 and thus to control the infrared switching by regulating input voltage or current. Several good reviews have reported recent progress in the development of VO_2 films as energy-efficient smart coatings [9–12]. Here, we discuss recent advances of VO_2 -based smart windows, by focusing on the strategies that enable the usage of VO_2 in ambient conditions. Therefore, in Section 1, a brief introduction of VO_2 is provided along with the strategies that regulate the TC performance of VO_2 in smart windows. In Section 2, recent developments on doping strategies that improve the TC performance of VO_2 materials are detailed. The electrothermal technique is introduced in Section 3, and recent research on the integrated VO_2 with other functional materials or structures is discussed in Section 4. Finally, an outlook of future developments will be given in Section 5.

2. Doping engineering

For application in smart windows, the working temperature of VO_2 is the first issue that should be considered as it is higher ($T_c = 68^\circ\text{C}$) than the room temperature (20–30 °C). To overcome this, elemental doping has been used to reduce the value of T_c . To date, elemental doping is the most efficient strategy to lower T_c and to modify the optical properties of VO_2 . Commonly, doping with high-valence cations, such as W^{6+} [17–19], Mo^{6+} [20,21], Nb^{6+} [22,23], and Ta^{5+} [24], or doping with monovalent atoms (H^+ [25,26]) can increase the carrier concentration and thus decrease T_c . For comparison, low-valence metal ions including Cr^{3+} [27,28] and Al^{3+} [29,30] are used to increase T_c . Moreover, doping with certain elements is proved to be a feasible method to boost the TC properties of VO_2 films including T_{lum} and ΔT_{sol} .

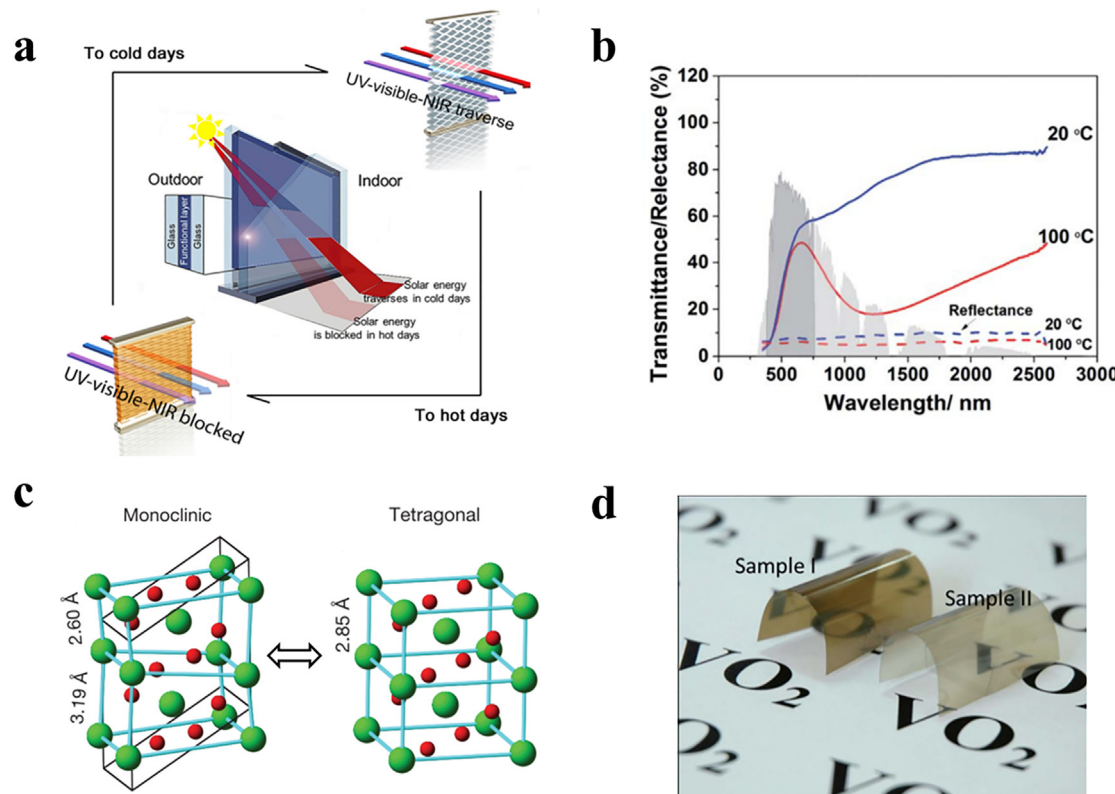


Fig. 1. VO_2 -based smart windows. (a) Schematic working mechanism of VO_2 as functional layers for smart windows. (b) Transmittance/reflectance spectra of thermochromic VO_2 film at 20 °C and 100 °C. (c) Atomic structures of monoclinic and tetragonal (rutile) phases of VO_2 (V, green spheres; O, red spheres). (d) Photos of flexible VO_2 films with high (sample I) and low (sample II) contents of VO_2 . The figures were reproduced with the permissions from (a) Ke et al., Elsevier [13], (b) Chen et al., Royal Society of Chemistry [14], (c) Budai et al., Springer Nature [15], and (d) Gao et al., Royal Society of Chemistry [16].

Table 1Elemental doping to tailor T_c and the thermochromic properties of VO_2 films.

Group	Dopant	Doping level (at.%)	T_c (°C)	T_{lum} (%)	ΔT_{sol} (%)	Ref.
Metal	W	0.7	42.7	61.7	11.7	[33]
	Nb	5.77	25	-	-	[23]
	B	6	28.1	54.3	12.5	[41]
	Mg	3.8	-	54.2	10.6	[45]
Non-metal	Ti	1.1	66.9	53	17.2	[48]
	F	2.93	35	48.7	10.7	[52]
	Co-doping	W + Sn	1.6 + 1.9	26	41.1	[55]
	W + Mg	2 + 4	35	81.3	4.3	[56]
Co-doping	W + Sr	0.9 + 11.9	29.3	61	5.2	[57]
	Fe + Mg	9.2 + 3	38.2	42.1	12.8	[58]

-' means data not available.

developed a facile and reproducible carbo-thermal method to synthesize highly crystallized Nb-doped VO_2 powder and then investigated the effects of Nb doping. From 0 to 5.77 at. % Nb doping, the T_c was reduced from 70 to 25 °C. The Nb-doped VO_2 powder consisted of 54 wt. % of the monoclinic phase and 46 wt. % of the rutile phase at the room temperature (Fig. 2c), which indicated its potential as TC films for smart windows. The recent study performed by Ersundu et al. [35] compared the effects of W and Nb on thermal, structural, and optical properties of the VO_2 film. They found that both W and Nb doping could reduce the T_c and improve the T_{lum} , but decrease the ΔT_{sol} values.

Compared with the aforementioned substitutional doping, boron (B) with a small atomic radius can be doped in interstitial sites of the VO_2 structure [36]; for this system, the reduction of T_c was predicted at a rate of 83 °C/at. % by Zhang's calculations [37], providing the feasibility for room-temperature smart windows. Banerjee's group [38] developed a novel post-synthesis approach to prepare B-doped VO_2 nanobeams. The structure analysis proved that doped B atoms were incorporated within interstitial sites (specifically the tetrahedral holes of the rutile phase) of VO_2 . Density

functional theory (DFT) calculations also indicated that the incorporation of B preferred the interstitial positions rather than substitutional sites. The incorporation of B helped to stabilize the rutile phase rather than the monoclinic phase, resulting in the decrease of T_c . However, the T_c was reduced by B doping at a rate of ~10 °C/at. % (Fig. 2d and e), which was far smaller than the prediction in Zhang's work [37]. In another study, they compared the effects of substitutional W and interstitial B dopants on the properties of the VO_2 system [39]. Both dopants could decrease the T_c and increase the transformation width, but the observed trend for the hysteresis was different. For undoped VO_2 , the hysteresis was strongly dependent on the particle size; this size effect could be deactivated after W or B doping (Fig. 2f). Recently, Hajlaoui et al. [40] fabricated B-doped VO_2 films via pulsed laser deposition and detected that B doping could cause a dramatic reduction in T_c at a rate of 31.5 °C/at. %. Lv's group [41] investigated the TC performance of B-doped VO_2 films. At 6.0 at. % B doping, a minimal T_c of 28.1 °C and a desirable performance of T_{lum} and ΔT_{sol} for smart windows could be achieved. Notably, there is a big difference of the B doping efficiency between the experimental results and the simulated value. In Zhang's model, the numerical method could deduce the qualitative trends on illustrating the ground-state properties of VO_2 , but ignored the dynamic correlation effects which significantly influenced the excited-state features and the value of T_c [40]. In addition, Zhang et al. assumed that the structure of B-doped VO_2 was fully relaxed, which was not consistent with experimental B-doped VO_2 films.

2.2. Modifying thermochromic properties

Besides the effective tunability of doping on T_c , some dopants (such as Mg and Ti) are beneficial for the enhancement of optical properties of VO_2 . Granqvist's group [42–44] studied the effect of Mg doping on the T_c and optical properties including luminous transmittance, absorption, and optical bandgap. The T_c was slightly decreased by 3 °C/at. % in Mg-doped VO_2 films fabricated by

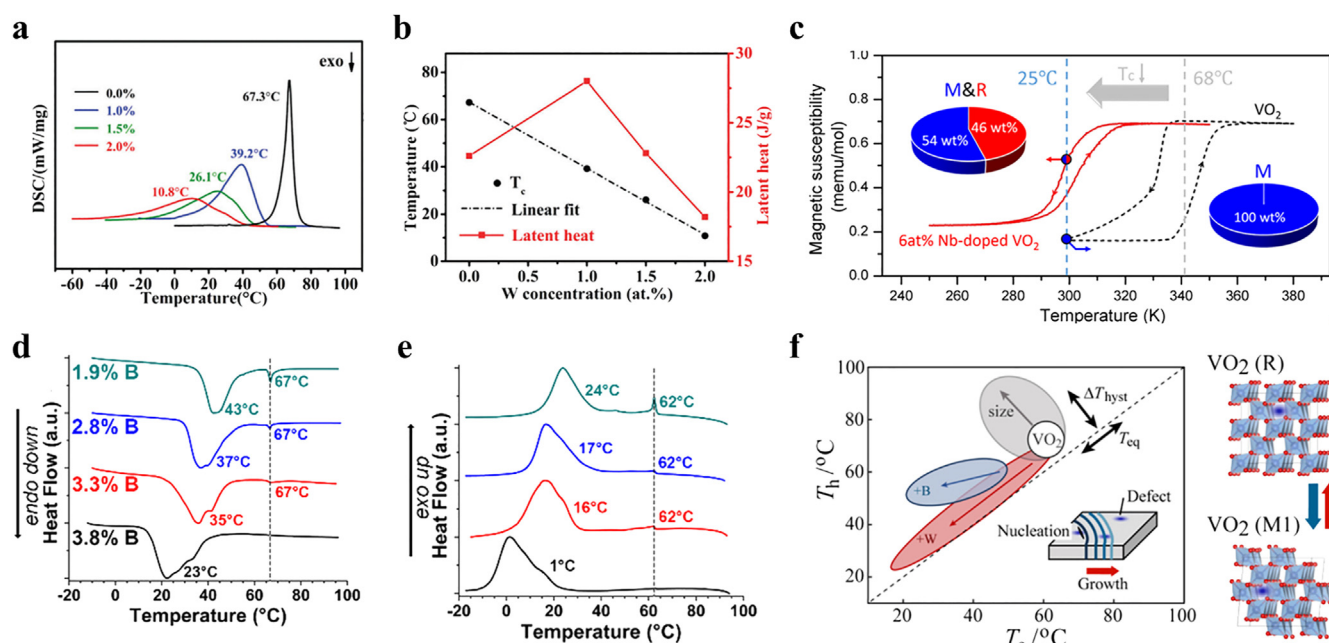


Fig. 2. Property of doped VO_2 films. (a) DSC curves, (b) T_c and latent heat values at varied W contents of W-doped VO_2 . (c) Magnetic susceptibility versus temperature hysteretic curves of undoped and Nb-doped VO_2 . DSC curves in the (d) heating and (e) cooling processes of VO_2 at different boron (B) contents. (f) The schematic diagram of doped VO_2 , showing the effects of W doping, B doping, and size of VO_2 on the phase transition temperatures and hysteresis widths. The dashed line depicts zero iso-hysteresis. The figures were reproduced with the permissions from (a–b) Shen et al., Royal Society of Chemistry [32], (c) Guan et al., American Chemical Society [23], (d–e) Alivio et al., American Chemical Society [38], and (e) Yano et al., American Chemical Society [39].

sputtering, whereas the T_{lum} was enhanced because of the widening of the optical bandgap. This widening (from 2.0 to 2.4 eV at 3.8 at. % Mg doping) was also reported by Gao's group [45] for Mg-doped nanoparticle composite foils. These results infer that the improvement of luminous transmittance could be achieved by doping elements that possess a larger bandgap than VO₂ in their oxide. Panagopoulou et al. [46] achieved a higher efficiency after Mg doping with reduced T_c and detected better TC properties for Mg-doped VO₂ on the ZnO/glass substrate than that on the SnO₂/glass. In a recent effort, the fabricated Mg-doped VO₂@ZrO₂-based films had optimized T_{lum} (52.4%) and ΔT_{sol} (7.1%) [47]. Besides Mg doping, Ti doping is another effective strategy for modifying the TC performance of VO₂ films because of a similar electronic structure and ionic radius. Gao's group [48] observed simultaneous improvements in both T_{lum} and ΔT_{sol} after compositing Ti ≤ 3 at. % within VO₂ composite foils. Similarly, zirconium (Zr) with the same valence and similar structure to V was determined to be an effective dopant for enhancing both T_{lum} and ΔT_{sol} with a slight decrease in T_c [49].

Besides the substitutional doping of vanadium sites in VO₂ structure, fluoride (F) was chosen to substitute the oxygen sites [50,51]. Dai et al. [52] prepared F-doped VO₂ nanoparticles with depressed T_c of 35 °C at 2.93 at. % F. F doping retained excellent TC properties and modified the color of the derived VO₂ composite film. Abdellaoui et al. [53] carried out the first-principles calculations using the HSE06 functional theory to study the energetic, electronic structure and optical properties of F-doped VO₂. They concluded that F doping resulted in decreasing the cell volumes and increasing the optical absorption, which matched well with the experimental results of Dai's work. Riapanitra et al. [54] synthesized F-doped VO₂ nanoparticles via a hydrothermal process at a supercritical temperature of 490 °C. They reported that the particle size decreased as the F doping level increased. At 0.13 at. % F doping, the T_c of the VO₂ film was reduced from 64 to 48 °C, and the film demonstrated a pronounced TC property, revealing its suitability for smart windows.

2.3. Co-doping

In addition to single-element dopants, co-doping with two elements, e.g. W–Mo [59,60], W–Nb [61], W–Zr [49], Fe–Mg [58], and Mg–F [53], was also conducted for simultaneous improvements of at least two aspects of properties. W is commonly used as one of co-doping elements because of its efficient reduction of T_c . The other elements for co-doping have been also studied including F [51], Mo [59,62], Nb [61], Zr [49], Mg [56], Sr [57], and Sn [55]. Long's group [56] conducted W/Mg co-doping to achieve high T_{lum} and low T_c for energy-saving smart windows. Dietrich et al. [57] investigated the impact of simultaneous W–Sr co-doping on the performance of VO₂ films. They found that W–Sr co-doping generated synergistic effects in reducing T_c because of W addition and bandgap widening originated from Sr incorporation (Fig. 3a and b). Similarly, Kim et al. [61] fabricated W– and Nb–co-doped VO₂ films and reported that the T_c could be well regulated to the room temperature (27 °C) after co-doping. Their co-doped VO₂ films exhibited desirable ΔT_{sol} of 18% and T_{lum} of 40%, which were suitable for smart window applications. Zhao et al. [55] found that Sn–W co-doping could significantly lower the T_c (less than 20 °C), boost the T_{lum} , and retain a good ΔT_{sol} (Fig. 3c and d). The enhancement of T_{lum} could be attributed to the lower refractive index (n) and extinction coefficient (k) in the visible range accompanied with the increased optical bandgap after Sn–W co-doping. Besides co-doping with W, some researchers explored the co-doping effect of Mg and other dopants. First-principles calculations conducted by Abdellaoui et al. [53] showed that Mg/F co-

doping could cause large gap widening in VO₂, which was beneficial to the improvement of T_{lum} . Ji et al. [58] prepared Fe/Mg–co-doped VO₂ films and determined the synergistic effect of Fe and Mg doping on the excellent TC performance of VO₂ films.

In short, elemental doping has proved to be a powerful and multifunctional technique to tune the properties of VO₂; it can not only tailor the T_c but also boost the T_{lum} and ΔT_{sol} of VO₂. The W dopant is considered as the most efficient one to lower the T_c in elemental doped VO₂ systems. Synergistic effects on the TC performance can be observed in doped VO₂ with some elements including Mg, Ti, F, Zr, and co-doped VO₂ systems such as W/Mg, W/Nb, and Fe/Mg. Significantly, these doped VO₂ systems can simultaneously lower T_c , increase T_{lum} , and improve ΔT_{sol} , which are crucial for smart windows of VO₂ films in ambient conditions.

3. Electrothermal technique

As we know, the MIT process of VO₂ is sensitive to ambient temperature; thus, researchers have allocated major efforts on tuning the T_c of VO₂ to approach the room temperature; however, sometimes the optical properties are affected in an undesirable way accompanied with the modification of T_c . In recent years, external voltage or current source was introduced to trigger the MIT in VO₂ because of its accessibility and controllability. For example, Bae et al. [63] applied a bias voltage of 0.34 V to trigger the MIT of a single VO₂ nanowire. By carefully regulating the number and amount of voltage pulses under low bias voltage, multiple retainable resistances were achieved for memristors. However, the phase transition mechanism under voltage remains highly debatable. Two mechanisms have been proposed to explain the voltage-induced MIT in VO₂: structural changes induced by Joule heating (thermal) and field-assisted carrier generation (electrical). Both mechanisms have received numerous experimental and theoretical supports. Zimmers et al. [64] observed homogeneous heating across micron-sized VO₂ channels after a DC voltage or DC current was applied, and the local temperature could reach up to the transition temperature; thus, they confirmed that Joule heating dominantly induced the insulator-metal transition in VO₂. Radu et al. [65] observed that the switching voltage strongly depended on the ambient temperature. The required power to trigger the MIT of the VO₂ device linearly declined on rising temperature; this evidence obviously supported the Joule heating mechanism, which was not involved in a pure field-induced transition. Yoon et al. [66] found that the carrier density of the VO₂ film device was closely related with the ambient temperature and device length. They observed that the electric field effect would dominantly activate the MIT of VO₂ as the device length was significantly shortened. Recently, Farjadian and Shalchian [67] proposed a comprehensive hybrid electrothermal model to comprehend the voltage-driven MIT in VO₂ materials. This model was verified by the experimental data of the I–V characteristics and hysteresis behaviors from both planar and vertical VO₂ structures. Based on this hybrid model, they predicted that the dominant mechanism varied from the Joule heating model to the field-assisted Mott transition model by reducing the VO₂ layer thickness from 250 μm to few 100 nm.

Despite the complicated mechanism of voltage-induced MIT in VO₂, the electrothermal method has been widely used in different VO₂-based devices. Zou's group [68] dynamically investigated voltage-triggered MIT of the VO₂ crystal film which was conjugated to an Al₂O₃ insulator substrate. They observed the temperature dependence of threshold voltages, revealing that the Joule heating effect was mainly responsible for the voltage-driven MIT. However, the triggering voltage (400–800 V) of a macro-VO₂ film was too high to use in real-life VO₂ devices such as smart windows. Thus, considering the required large power consumption to utilize the

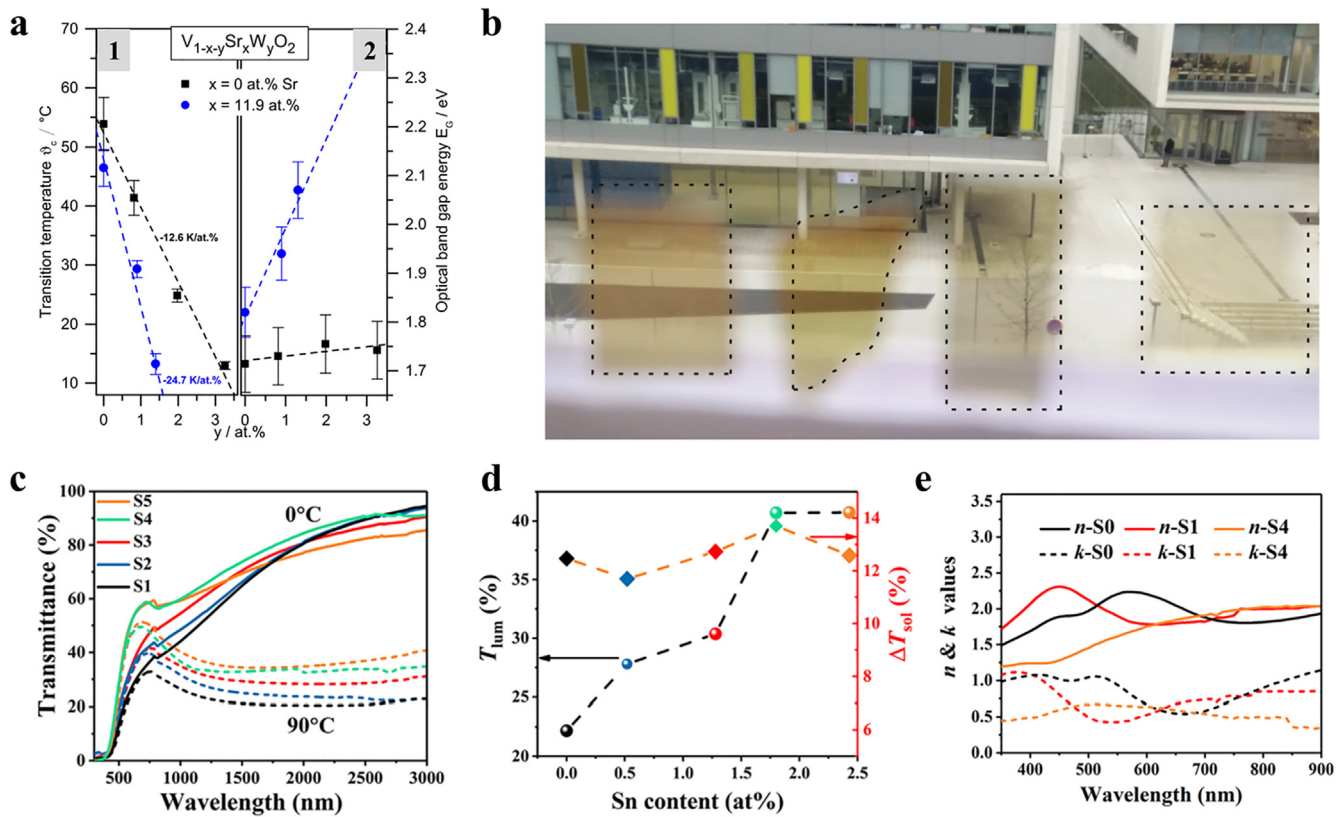


Fig. 3. Performance of co-doped VO₂ films. (a) The phase transition temperatures (1) and bandgap values (2) versus W concentrations of V_{0.881-y}Sr_{0.119}W_yO₂ films. (b) Photos of four different doped films with the same thickness of about 100 nm: undoped VO₂ (left), V_{0.98}W_{0.02}O₂, V_{0.881}Sr_{0.119}O₂, and V_{0.872}Sr_{0.119}W_{0.009}O₂ (right). The increasing bandgap caused a color change from brown to greyish. (c) Transmittance spectra, (d) T_{lum} and ΔT_{sol} , and (e) optical parameters (n and k) in the visible range of Sn–W–co-doped VO₂ films with varied Sn contents. S0, S1, S2, S3, S4, and S5 refer to undoped VO₂, W_{0.01}V_{0.99}O₂, W_{0.01}Sn_{0.01}V_{0.98}O₂, W_{0.01}Sn_{0.03}V_{0.96}O₂, W_{0.01}Sn_{0.05}V_{0.94}O₂, and W_{0.01}Sn_{0.08}V_{0.91}O₂, respectively. The figures were reproduced with the permissions from (a–b) Dietrich et al. [57], AIP publishing, and (c–e) Zhao et al. [55], American Chemical Society.

Joule heating effect of a macro-sized VO₂ film, researchers are in the thought that transparent-conductive materials can be introduced to electro-TC VO₂ devices as the resistive element to produce Joule heat and transfer it to the functional VO₂ layer. Specifically, the influence of substrates with different kinds of transparent-conductive layers has been studied in electrically induced MIT for smart windows. Compared with passive response to the ambient temperature, active control by electrical voltage can be a good option for smart windows.

Li et al. [69,70] deposited VO₂ nanoparticles on ITO or glass coated with Ag nanowires to achieve the electrothermal-induced MIT and infrared switching. Ag nanowires or ITO served as heaters in the double-layered VO₂ structures (Fig. 4a). It can be observed that the infrared transmittance of VO₂ films is declined as the applied voltage increases. When the applied voltage across the electrodes reached above the threshold value, the sufficient Joule heat that was generated by Ag nanowires or ITO was transferred to VO₂ and caused complete MIT. For VO₂/ITO double-layered films, 15 V was high enough to induce a complete MIT (Fig. 4b) and cause a large infrared modulation of 38.5% at 1.55 μm wavelength (Fig. 4c).

Hao et al. [71] fabricated VO₂ on an F-doped SnO₂ (FTO) conductive glass substrate and developed an FTO/VO₂/FTO structure to study the electric field-triggered MIT and optical modulation of the VO₂ film. The FTO glass allowed the higher temperature fabrication (550 °C) of VO₂ than the ITO glass, and the deposited VO₂ film was formed with a better film quality. The threshold voltage required to induce the complete MIT declined significantly with rising temperature (Fig. 4d and e), reflecting a distinct feature of the Joule heating process. Recently, Xu et al. [72] reported one-

step deposition of the VO₂ thin film on an FTO/glass substrate. Because of the resistive heating derived from the FTO layer, the infrared switching of the VO₂ thin film could be dynamically regulated and a contrast of ~48% at 1.6 μm wavelength (Fig. 4f) was achieved.

Zou's group [73] deposited VO₂ on a highly conductive n-type GaN/Al₂O₃ substrate via a molecular beam epitaxy process. They carefully modulated the infrared transmittance of VO₂ films by dynamically controlling the external voltage applied on the two-terminal VO₂/GaN device (Fig. 4g). As the bias voltage gradually increased to the threshold value of 5.0 V, the infrared transmittance decreased dramatically; when the bias voltage was removed, it could recover to its initial state (Fig. 4h). Besides this optical transmittance modulation, an optical memory behavior of the VO₂ device could be derived from its hysteretic effect. As shown in Fig. 4i, series of balance states could be obtained by applying a continuous pulsed voltage, with certain recorded infrared transmittance. Thus, an 'electrical writing-optical reading' mode of the VO₂ device was triggered, reflecting an optical memory behavior.

Skuza et al. [74] investigated the electro-thermal control of aluminum-doped zinc oxide (Al:ZnO, denoted as AZO)/VO₂ multilayered films. They observed that a small electric field across the AZO film could produce the required heat to induce the MIT of VO₂ films (see the change of Raman intensity in Fig. 5a). The converted heat from the electric power was proportional to the square of applied voltages (Fig. 5b), revealing the Joule heating effect. This electrically induced MIT in VO₂ had a hysteresis-type behavior during the heating and cooling process (Fig. 5c). Besides, the AZO film acted as a capping layer to prevent the oxidation of

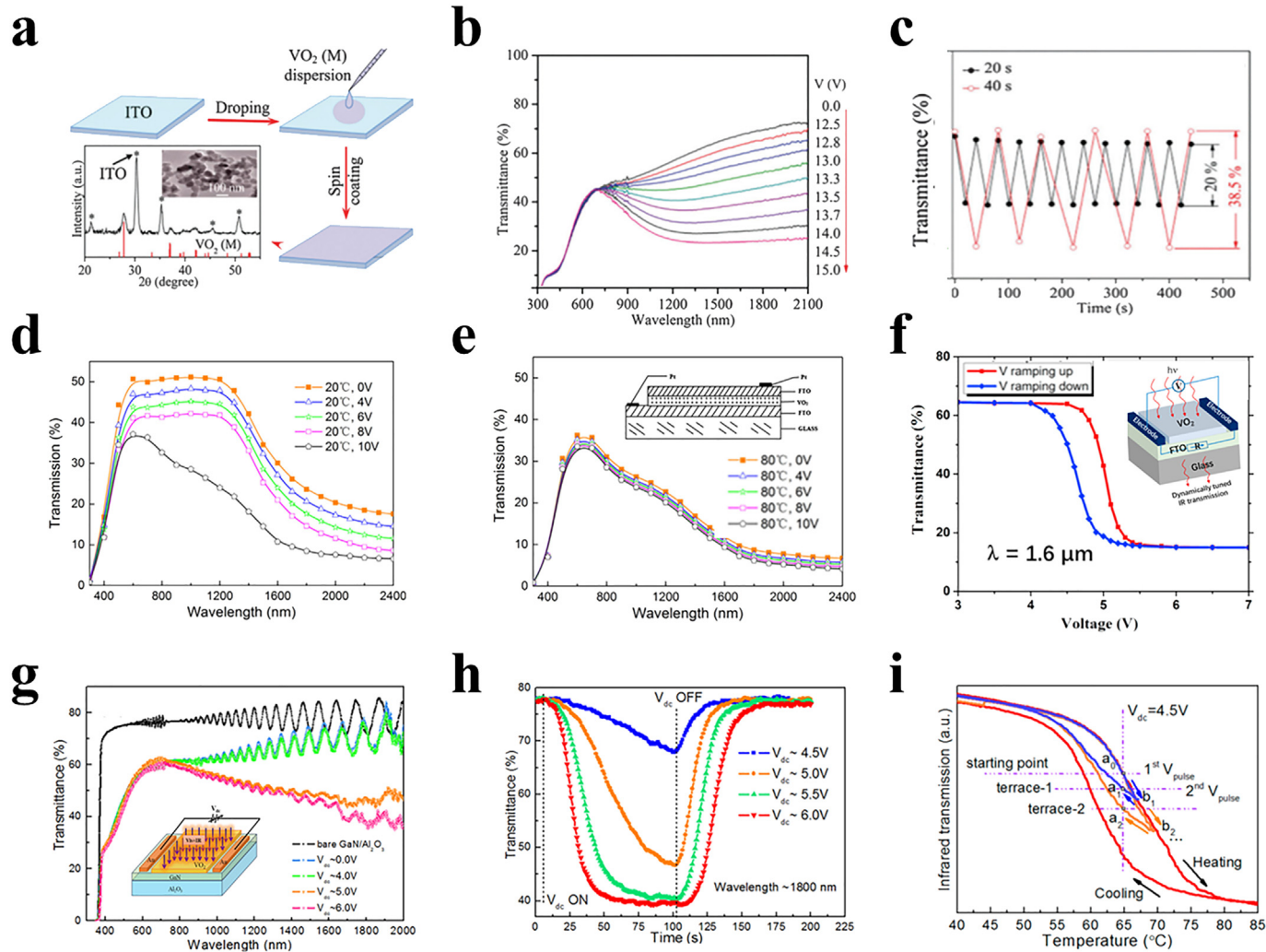


Fig. 4. Electro-thermal-induced MIT in VO₂ films on ITO, FTO glass, and GaN/Al₂O₃ substrates. (a) The schematic fabrication process, transmission electron microscope (TEM) image, and X-ray diffraction (XRD) pattern of VO₂ on the ITO glass. (b) Voltage-dependent transmittance spectra of the VO₂/ITO device. (c) Infrared switching performance of the VO₂/ITO device at 1.55 μm wavelength with 20 and 40 s pulse durations under pulse voltage of 15 V. Voltage-dependent transmittance spectra of the FTO/VO₂/FTO device at (d) 20 °C and (e) 80 °C. The inset shows the structure of the FTO/VO₂/FTO device. (f) Two-terminal device structure under applied voltage. (g) Voltage-dependent transmittance at 1.6 μm wavelength of the VO₂/FTO device and the inset refers to the device structure. (h) The infrared transmittance of VO₂/GaN/Al₂O₃ at 1.8 μm wavelength versus time under dynamic bias voltages. (i) The transmittance-temperature hysteresis curves of VO₂/GaN/Al₂O₃ at 1.8 μm wavelength, which suits it for memory devices. The figures were reproduced with the permissions from (a–c) Li et al. [70], Royal Society of Chemistry, (d–e) Hao et al. [71], Elsevier, (f) Xu et al [72], Elsevier, and (g–i) Fan et al. [73], American Chemical Society.

VO₂ to V₂O₅ and caused a slight decrease in the transition temperature (5–10 °C). Zhang et al. [75] studied various optical responses of hybrid multilayer VO₂/AZO films and the influence of number and configuration of the AZO layer on the performance of the device. From the reflectance and absorption spectra, they found that AZO became an ordinary substrate at the buffer layer, whereas it served as a highly absorptive dielectric film at the capping layer and caused the temperature-dependent redshift of the absorption peak in the near-infrared region. Furthermore, they fabricated ladder-like electrodes on hybrid VO₂/AZO heterojunctions to study the effects of planar and vertical electrode distance during the Joule heating process. As shown in Fig. 5d, three voltages of V₁, V₂, and V₃ were applied to different electrodes for the Al₂O₃/AZO/VO₂ film, where the infrared transmittance decreased with the input voltage. As for V₁, the voltage of transition (V_{MIT}) and the saturation voltage were about 8.5 V and 9.5 V, respectively (Fig. 5e). The saturation voltages of V₂ and V₃ increased because of the larger area and horizontal electrode distance of the device (Fig. 5f). As per the Joule heat equation, Joule heat could be estimated based on the I–V

curves (Fig. 5g). Thus, Joule heat for V₂ or V₃ was far more than that for V₁ under similar duration, which was due to larger surface area. Besides, the saturation voltage of V₁ was smaller than that for the VO₂/ITO device in Li's work [70], which could be attributed to the ladder-like configuration of the electrode. Xiao et al. [76] specifically detected the electro-optical properties of the vertical AZO/VO₂/AZO sandwiched structure. When a certain voltage of 7.5 V was applied to both sides of the structure at 20 °C, the MIT was completely induced, and the infrared modulation could approach 28% at the wavelength of 1500 nm. The required voltage to trigger the MIT decreased with increasing the ambient temperature. Zhang et al. [77] fabricated VO₂ films with small hysteresis width on the AZO glass substrate at low temperature. The MIT of the VO₂ film with a low T_c of 48 °C could be triggered by Joule heating, which was originated from the AZO conductive layer. This way may be more convenient than the traditional heating method equipped with an external heating plate.

Zou's group [78] fabricated free-standing single-walled carbon nanotubes (SWNTs)/VO₂/mica hierarchical films with good TC

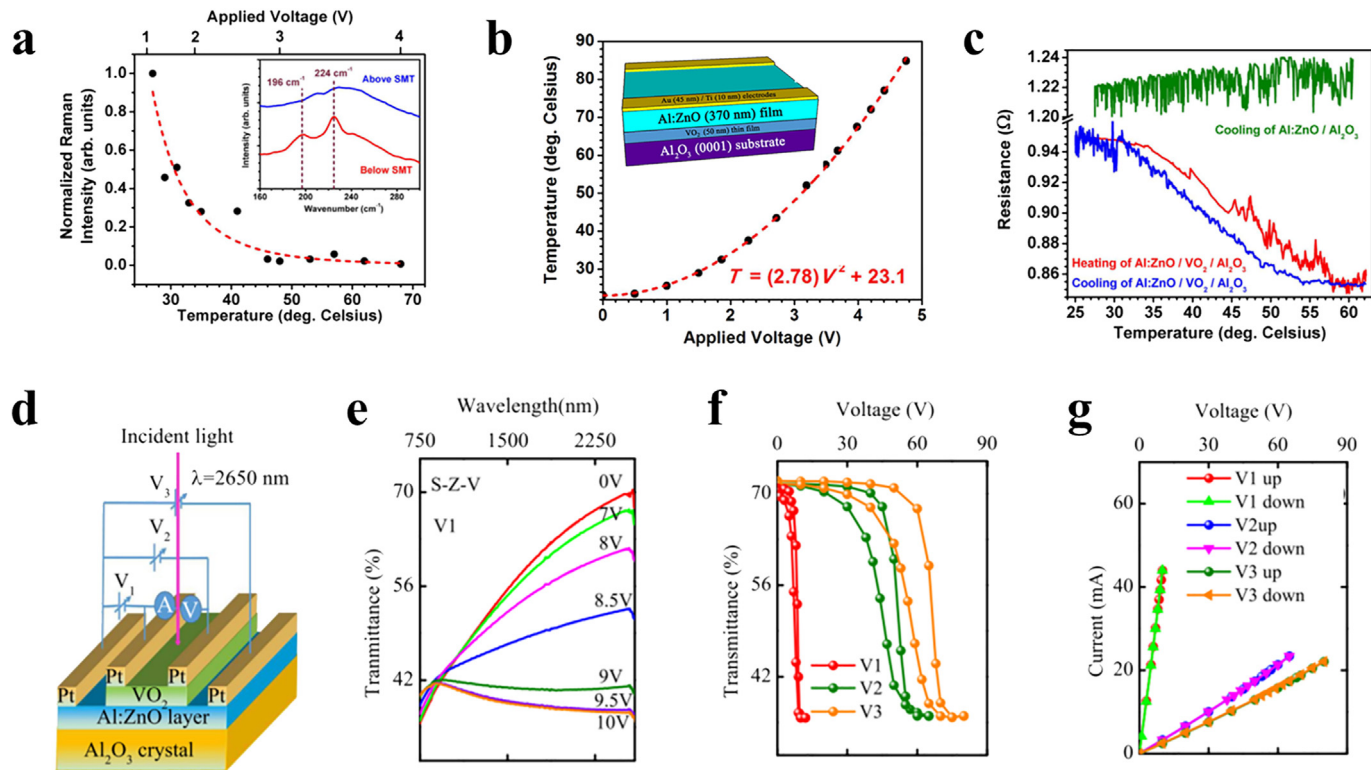


Fig. 5. Electrothermally induced MIT in VO_2/AZO multilayer compositions. (a) The normalized Raman intensity as a function of temperature when voltages are applied to the AZO/ $\text{VO}_2/\text{Al}_2\text{O}_3$ multilayer film and the inset shows the 196 cm^{-1} and 224 cm^{-1} Raman modes used to track the intensity variations with temperature. (b) The function of temperature versus applied voltage, reflecting a parabolic relation, the inset shows the schematic structure of the AZO/ $\text{VO}_2/\text{Al}_2\text{O}_3$ multilayer. (c) Resistance versus temperature hysteresis curves of the AZO/ VO_2 multilayer film, in comparison with that of the AZO/ Al_2O_3 film without the VO_2 layer. (d) The scheme of the $\text{Al}_2\text{O}_3/\text{AZO}/\text{VO}_2$ (denoted as S-Z-V) device. (e) The transmittance spectra of the S-Z-V device under different voltages. (f) The hysteresis curves of transmittance at 2650 nm versus voltage of the S-Z-V device. (g) The I-V curves of the S-Z-V device. The figures were reproduced with the permissions from (a–c) Skuza et al. [74], Springer Nature, and (d–g) Zhang et al. [75], Springer Nature.

performance. As shown in Fig. 6a, highly transparent and flexible mica pieces were used as substrates to grow the VO_2 film, whereas ultrathin SWNTs acted as heaters on the surface. Because of the weak van der Waals bonding force between muscovite mica layers, the SWNTs/ VO_2 /mica film could be easily peeled off (the upper inset of Fig. 6b) and transferred to other flexible substrates. By applying different bias currents, the infrared transmission could be carefully controlled as a result of local Joule heating (Fig. 6b). Cheng's group [79] deposited VO_2 nanoparticles on a flexible ITO/polyethylene terephthalate (PET) substrate via a doctor blade process at the room temperature (Fig. 6c and d) and achieved controllable infrared switching performance of flexible VO_2 films by applying external voltages. With increasing the applied voltage, the infrared transmittance decreased accordingly and finally stabilized under a threshold voltage; the induced MIT could be dynamically regulated by the input voltage in a step-like increasing trend or pulse shape. The authors further evaluated the input power consumed to trigger the MIT and predicted the minimal power to maintain the MIT performance in an energy-saving way. Importantly, as observed in Fig. 6e, the input power, which was required to maintain the maximum infrared blocking performance, could be significantly reduced to a smaller value (15% of the initial value to trigger the MIT) because of the hysteretic behavior of MIT in VO_2 . This finding was significant for energy-saving VO_2 -based devices. Besides, the VO_2 nanoparticle films exhibited superior flexibility as the optical properties underwent no obvious deteriorations after 10,000 bending cycles.

Electrothermal techniques enable the adaptive MIT occurrence in VO_2 materials at different ambient temperatures. It is known that plasmonic materials such as titanium nitride (TiN) can convert the

radiation to local heat when the irradiation wavelength coincides with the plasmon resonant wavelength. Chu et al. [80] used an infrared irradiation source of 975 nm (in accordance with the plasmon resonant wavelength of TiN nanoparticles) to excite TiN nanoarrays via plasmon resonances. The subjected plasmonic TiN nanoparticles absorbed near-infrared radiation, converted it to heat, and induced the MIT of VO_2 in the VO_2/TiN bilayer. By a decent excitation, the VO_2/TiN smart coating could block 70% of infrared radiation at 28°C under strong illumination conditions, whereas it became infrared transparent at 20°C or under weak illumination. Thus, the near-infrared transmittance could be well regulated in accordance with the ambient temperature and illumination intensity.

4. Integration techniques

4.1. Integration with transparent coatings

For VO_2 -based smart windows, integrated structures with inorganic or organic materials are considered to boost the TC performance of VO_2 with diverse functionalities. For example, it would be significant to equip the ordinary glass windows with self-cleaning ability because air pollution can cause increasing costs to keep the glass windows clean. Photocatalysis technique is a cost-effective way which is capable of removing almost any type of organic air pollutants. Integration with photocatalysts can add self-cleaning property to smart windows.

Titanium dioxide (TiO_2) is introduced as a protective and functional layer for self-cleaning purposes in the multilayered structure of VO_2 because of its effective photocatalytic degradation of organic

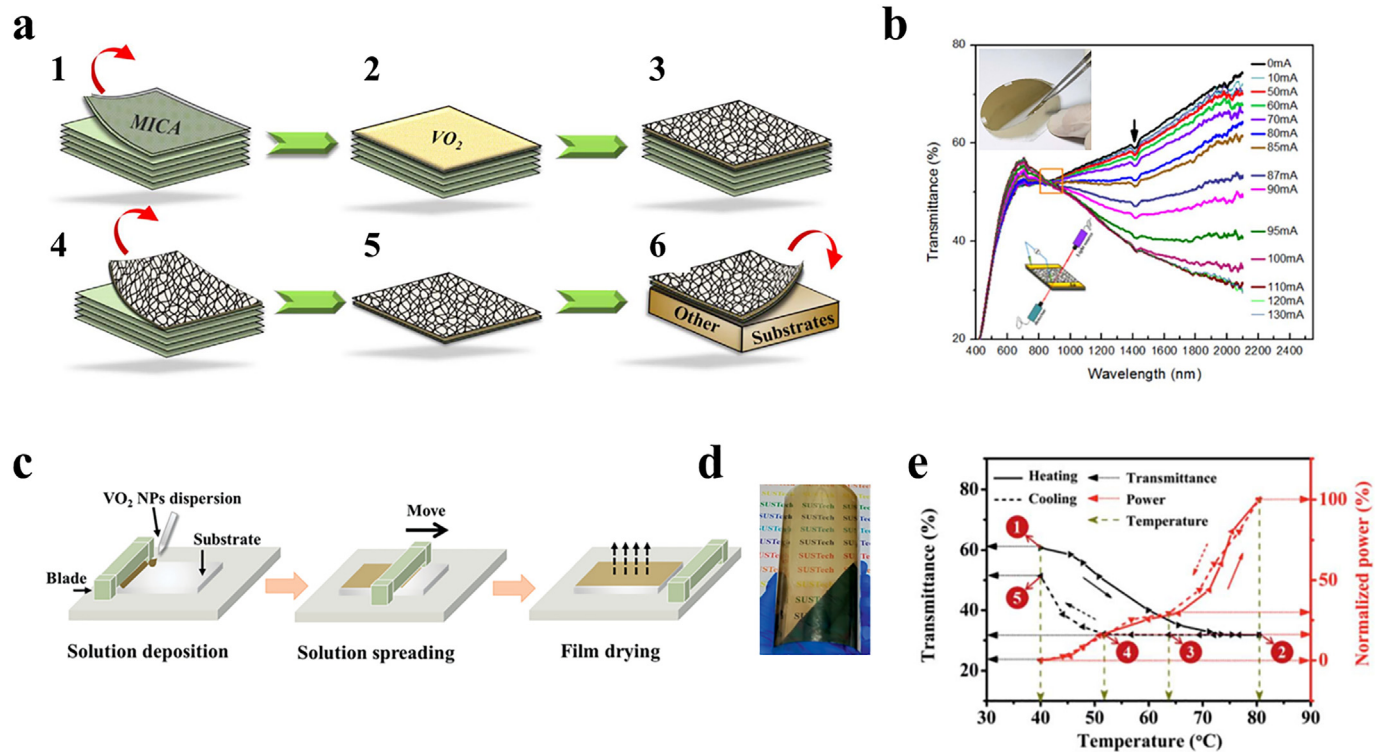


Fig. 6. Electrothermally induced MIT in flexible VO_2 -based films. (a) The fabrication process of the SWNTs/ VO_2 /mica film is as follows: (1) cleaning the surface of mica substrates, (2) growing VO_2 on mica, (3) covering SWNTs on the VO_2/mica bilayer, (4) peeling off the SWNTs/ VO_2/mica , (5) free-standing SWNTs/ VO_2/mica film, and (6) transferring to other substrates. (b) The transmittance spectra of the SWNTs/ VO_2/mica film with varied input currents and the insets show the peeled-off flexible SWNTs/ VO_2/mica film (upper) and the illustration of in situ optical measurement (lower). (c) The schematic of the doctor blade process to prepare the VO_2 nanoparticle composite film. (d) The photo of the synthesized flexible VO_2 nanoparticle composite film. (e) The function of normalized power versus temperature of the VO_2 film and corresponding transmittance-temperature hysteresis curves. The figures were reproduced with the permissions from (a–b) Chen et al. [78], Elsevier, and (c–e) Shen et al. [79], Royal Society of Chemistry.

contaminants [81,82]. Parkin's group [83] fabricated multilayered $\text{VO}_2/\text{SiO}_2/\text{TiO}_2$ films (Fig. 7a) via an atmospheric-pressure chemical vapor deposition process to develop an advanced bifunctional self-cleaning and energy-saving setup. The self-cleaning property obtained from the addition of the photocatalytic TiO_2 layer was comparable with the performance of commercial Pilkington Activ glass (Fig. 7b). Besides, many studies prove that TiO_2 can be used as antireflection coatings on the surface of the VO_2 layer to improve T_{lum} and ΔT_{sol} [84,85]. Top et al. [86] observed that VO_2/TiO_2 bilayer films (Fig. 7c) exhibited increased T_{lum} of up to 66% and a higher near-infrared transmittance modulation of up to 20% compared with bare VO_2 films. The addition of the TiO_2 top layer also resulted in enhanced wetting behavior through photo-induced superhydrophilicity (Fig. 7d). Lately, Ji et al. [87] reported synergistic TiO_2/VO_2 bilayer coatings with enhanced T_{lum} and photocatalytic activity. In their experiment, the TiO_2 photocatalytic layer admitted the indoor air cleaning responsibility. Consistent with other studies, the layer acted as an antireflection layer which improved the T_{lum} and ΔT_{sol} (Fig. 7e). Moreover, TiO_2/VO_2 bilayer coatings could degrade stearic acid by a photocatalytic process at an almost twice rate compared with that for single-layer TiO_2 (Fig. 7f). They analyzed that the underlying infrared-absorbing VO_2 film heated the TiO_2 and thus enhanced the photocatalytic air purification performance of TiO_2 . This pronounced synergy between the two layers in the TiO_2/VO_2 bilayer coating could pave the way for energy-efficient and self-cleaning windows. Recently, improved T_{lum} (55.4%) and ΔT_{sol} (11.3%) were investigated in VO_2 films coated with the TiO_2 layer with a unique nano-cone structure [88]. This moth eye-inspired nano-cone structure of the TiO_2 layer provided better angular and polarization independence than the planar TiO_2

antireflection layer (Fig. 7g and h), upgrading the value for VO_2 smart windows. This cone-like biomimetic structure was also studied by Long's group [89]. They developed a cost-effective and universal bottom-up technique to fabricate this biomimetic antireflection structure by using monolayer-assembled Ag nanowire (AgNW) as templates. The aligned crisscrossing AgNW nanomesh had randomly distributed cone-like peaks similar to the butterfly's wing, exhibiting high transparency due to the omnidirectional broadband antireflection. The VO_2/AgNW multilayer film demonstrated 70% reduction of omnidirectional reflectance and 37% improvement of T_{lum} with no sacrifice of the TC performance.

Another commonly used coating is SiO_2 because of its inert properties and antireflection effects [90]. First, SiO_2 coatings are introduced as a protective layer on the top of VO_2 to prevent the oxidation or intermediate antireflection layers in multilayered structures [91,92]. In Parkin's work [83] on the $\text{VO}_2/\text{SiO}_2/\text{TiO}_2$ multilayer structure, the $\text{SiO}_2/\text{TiO}_2$ bilayer served as antireflection coatings, whereas the sandwiched SiO_2 acted as a barrier layer that could prevent the diffusion of Ti^{4+} ions. To obtain an integrated VO_2 multilayer structure with an acceptable low refractive index within the visible range, Zhang et al. [92] fabricated the mesoporous SiO_2 layer with a refractive index ranging from 1.243 to 1.354 on the VO_2 film to improve the visible transmission (up to 80.0%) by reducing the total surface reflection of bilayer coatings.

Second, VO_2 -based core-shell structures, especially $\text{VO}_2@\text{SiO}_2$ core-shell nanoparticles [16,93], have been well investigated. This is because the effective medium theory indicated that a hybrid system consisting of highly dispersed VO_2 nanoparticles in dielectric hosts demonstrated enhanced optical performance [94]. Gao's group [16] has performed some studies on the $\text{VO}_2@\text{SiO}_2$ core-shell

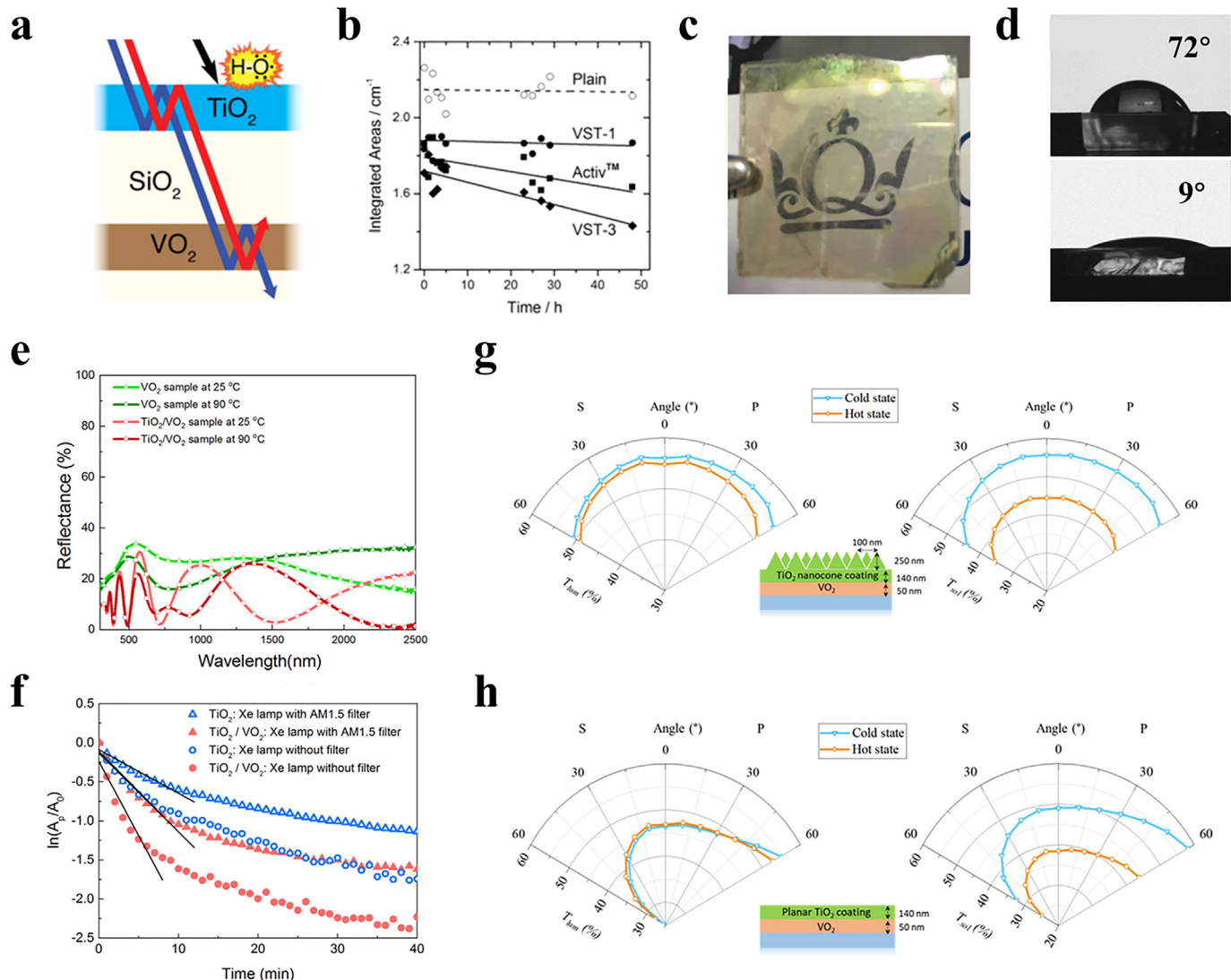


Fig. 7. Inorganic-inorganic VO_2/TiO_2 hybrid coatings. (a) Illustration of the $\text{VO}_2/\text{SiO}_2/\text{TiO}_2$ sandwiched structure. (b) Integrated areas of stearic acid under UV irradiation ($I = 4 \text{ mW/cm}^2$), revealing the photocatalytic ability of the $\text{VO}_2/\text{SiO}_2/\text{TiO}_2$ film. VST-1 and VST-3 refer to the $\text{VO}_2/\text{SiO}_2/\text{TiO}_2$ film with different deposition times of the VO_2 layer (1 and 3 min, respectively). (c) The photo of the VO_2/TiO_2 bilayer film. (d) Contact angle measurements: pictures of water droplets on the surface of the VO_2/TiO_2 bilayer film before and after the UV illumination (254 nm, 60 min). (e) Reflectance spectra of the VO_2 (53 nm) and TiO_2/VO_2 (297 nm/53 nm) bilayer film at 25 and 90 °C. (f) The scattered diagram of logarithm of the ratio of A_p and initial integrated area, A_0 , versus time. The initial photodegradation rates can be estimated via solid lines in (f). The simulated T_{lum} and T_{sol} of the VO_2 film with (g) TiO_2 nanocone coating and (h) planar TiO_2 coating under different angles and polarization states. P and S refer to p-polarized and s-polarized light, respectively. The figures were reproduced with the permissions from (a–b) Powell et al. [83], American Chemical Society, (c–d) Top et al. [86], Royal Society of Chemistry, (e–f) Ji et al., Elsevier [87], and (g–h) Liu et al. [88], Springer Nature.

structure and verified that the anti-oxidation and anti-acid abilities of VO_2 nanoparticles could be significantly improved by coating with a thin SiO_2 shell. By mixing $\text{VO}_2@\text{SiO}_2$ core-shell nanoparticles with well-dispersed mesoporous silicon nanospheres [95], the T_{lum} (from 62.29% to 71.02%) and ΔT_{sol} (from 0.7% to 14.31%) of VO_2 -based films can be simultaneously enhanced. Qu et al. [96] fabricated $\text{VO}_2@\text{SiO}_2$ dual-shell hollow nanospheres (DSHNs) via a process depicted in Fig. 8a. Different from the process of coating the SiO_2 shell on VO_2 cores in most core-shell structures, ammonium polyacrylate acted as a bifunctional template to form the SiO_2 shell and as a scaffold to immobilize the vanadium precursor (VO_2^{2+}) on the inner surface of SiO_2 shells because of electrostatic repulsion (Fig. 8b). The obtained $\text{VO}_2@\text{SiO}_2$ DSHN coating showed a good optical performance ($T_{\text{lum}} = 61.8\%$, $\Delta T_{\text{sol}} = 12.6\%$) as a result of its unique structure. Banerjee's group [97] developed an aqueous processing approach to obtain the VO_2 nanocomposite film and investigated the influence of the amorphous SiO_2 shell and

perfluorinated silane ligand shell on the optical property of the VO_2 composite film. The homogeneous thin films exhibited a high degree of visible transmittance and near-infrared modulation (Fig. 8c). Besides SiO_2 shells, TiO_2 [98], zinc oxide (ZnO) [99], and zirconium oxide (ZrO_2) [47] are also coated as shells on the surface of VO_2 to protect it from oxidation and offer functionalities to the VO_2 structure. In addition, SiO_2/VO_2 core/shell foils displayed distinct colors varying from red, green to blue, accompanied with high near-infrared modulation (Fig. 8d). A significant improvement (18.6%) of T_{lum} can be achieved in biomimetic SiO_2 nanosphere-patterned VO_2 thin films because of the antireflection effects [101].

Long's group [102] fabricated a series of periodic patterned VO_2 films for high-transparency smart windows. Liu et al. [103] designed a novel nanogrid structure of VO_2 -based films and demonstrated the best performance of T_{lum} (76.5%) and ΔT_{sol}

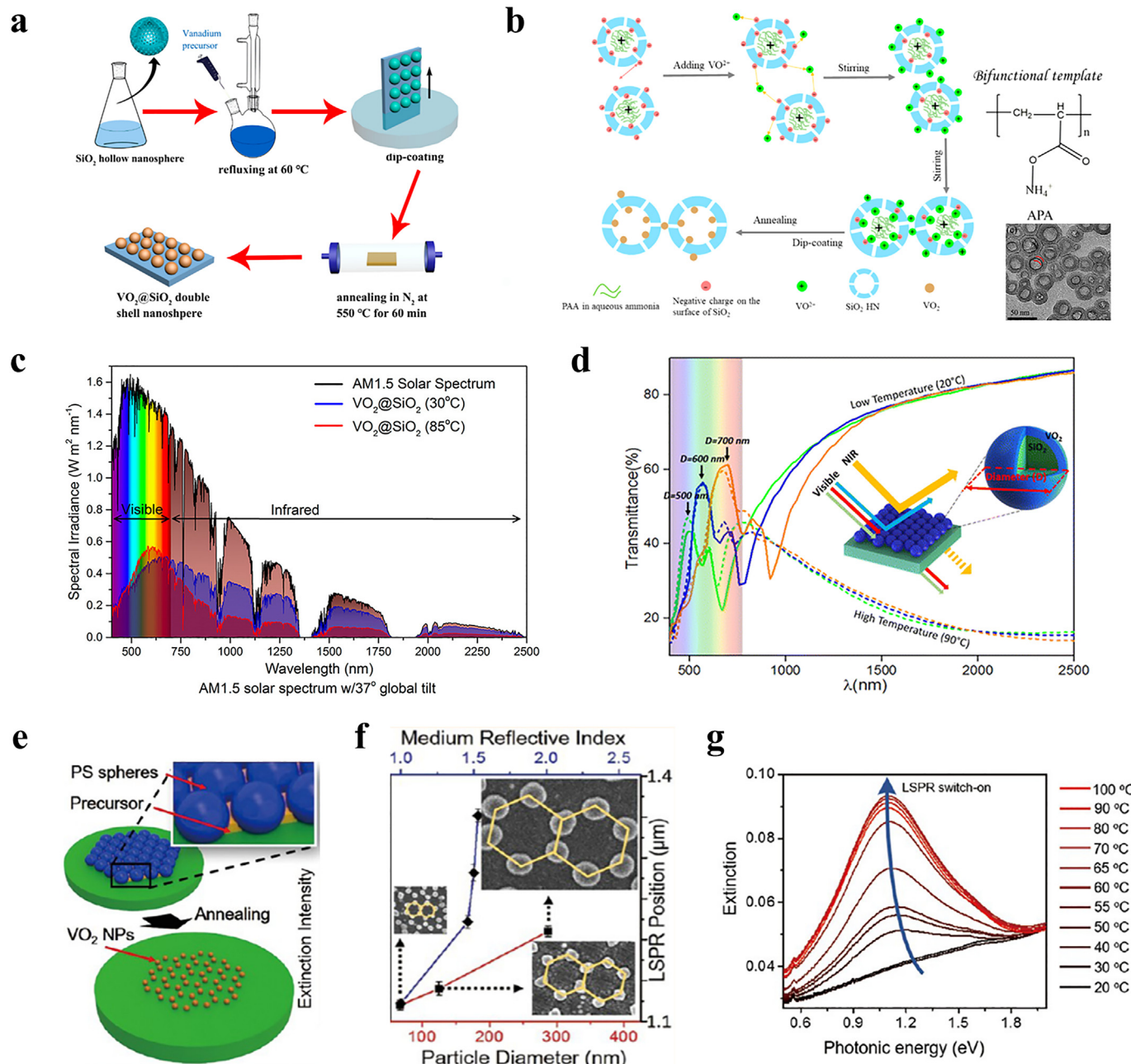


Fig. 8. $\text{VO}_2\text{-SiO}_2$ hybrid films. (a) The fabrication process of $\text{VO}_2\text{@SiO}_2$ DSHNs and coatings. (b) The formation process of $\text{VO}_2\text{@SiO}_2$ DSHNs due to electrostatic interactions and the inset image at the bottom right corner shows the morphology of $\text{VO}_2\text{@SiO}_2$ DSHNs. (c) The solar spectral irradiation of the $\text{VO}_2\text{@SiO}_2$ coating in the visible and near-infrared range at 30 °C and 85 °C, comparing with the AM 1.5 solar spectrum. (d) Simulated transmittance spectra of the SiO_2/VO_2 core-shell structure with different diameters. The colored region reveals the visible range from 370 nm to 770 nm. (e) The preparation scheme of 2D patterned VO_2 nanoparticles using polystyrene (PS) spheres as monolayer colloidal crystal templates. (f) The relationship between the LSPR position and the particle diameter/medium reflective index within the patterned VO_2 nanoparticle films. (g) The extinction spectra of VO_2 nanoparticle films, revealing the temperature-dependent LSPR intensity in the range of 20–100 °C. The figures were reproduced with the permissions from (a–b) Qu et al. [96], American Chemical Society, (c) Fleer et al. [97], American Chemical Society, (d) Ke et al. [100], American Chemical Society, and (e–g) Ke et al. [104], American Chemical Society.

(14.0%) in nanogrid structures of VO_2 via the finite difference time domain simulations. Their theoretical results were superior to previous results obtained in nano thermochromism, nanoporosity, and biomimetic nanostructuring. After that, a periodic micro-patterned VO_2 TC film was synthesized using screen printing meshes with improved T_{lum} (67%) and ΔT_{sol} (8.9%) compared with continuous films. Furthermore, Ke et al. [104] proposed a universal nanosphere lithography technique to develop two-dimensional ordered nanostructures. By tuning plasma etching duration and

viscosity of the precursor, series of nanoparticle, nanonet, and nanodome arrays with controllable periodicity could be fabricated (Fig. 8e). The localized surface plasmon resonance (LSPR) phenomenon on VO_2 nanoparticle arrays was studied and the position of LSPR was regulated from 1120 to 1350 nm through controlling the particle size of VO_2 arrays and the reflective index of the medium encapsulating VO_2 nanoparticles (Fig. 8f). More interestingly, LSPR intensity could be enhanced with dynamically increasing the temperature of nanoparticle arrays, which was due to intermediate

phase coexistence during the MIT (Fig. 8g). The result of this work highlighted that ΔT_{sol} might be improved by adjusting the intensity and position of LSPR.

4.2. Inorganic-organic hybrid structure

Hybrid VO₂ coatings with organic materials have attracted significant attentions because of their accessibility, low cost, and diverse functionalities, e.g. wettability and thermochromism [105,106]. To date, several TC organic materials are introduced for hybrid VO₂ structures [107]. Ultrahigh solar energy modulation and luminous transmission could be attained in one VO₂/hydrogel hybrid (Fig. 9a) [108]. This poly(N-isopropylacrylamide) hydrogel with a hydrophilic-to-hydrophobic phase transition of 32 °C presented large luminous modulation (ΔT_{lum}) of 29.7%. Thus, an unprecedented high ΔT_{sol} (34.7%) with moderate T_{lum} (62.6%) occurred by combining the luminous regulating organic matrix and infrared-regulating inorganic VO₂ nanoparticles in the VO₂/hydrogel hybrid (Fig. 9b). Similarly, a cobalt^{II}-based ligand

exchange TC system (CLETS) demonstrated TC behavior from nearly transparent to blue in response to heating, with reflected visible light modulation and color tunability [109]. In the CLETS/VO₂ hybrid film, an enhanced ΔT_{sol} of 20.82% could be reached because of the enlarged modulation in both visible (CLETS component) and near-infrared (VO₂ particles) regions (Fig. 9c). However, the CLETS/VO₂ hybrid suffered from the inevitable solvent evaporation in repeated heating-cooling cycles. To overcome this problem, non-volatile TC ionic liquid-nickel-chlorine complexes [110] were utilized as the matrix for VO₂ nanoparticles; the hybridizing effect resulted in the increment in the magnitude of ΔT_{sol} and T_{lum} . Lately, embedding tungsten-doped VO₂ nanoparticles in thermoresponsive 2-hydroxy-3-butoxypropyl starch resulted in distinct ΔT_{sol} of 34.3% and high T_{lum} (53.9%) [111].

Flexibility is one of the demanded features of VO₂ films for different types of glass panels. Long's group [13] developed adaptive and plasmonic poly(dimethylsiloxane) (PDMS)-supported VO₂ composite films with kirigami-inspired reconfigurable metastructures. By dispersing VO₂ particles in the elastomer PDMS

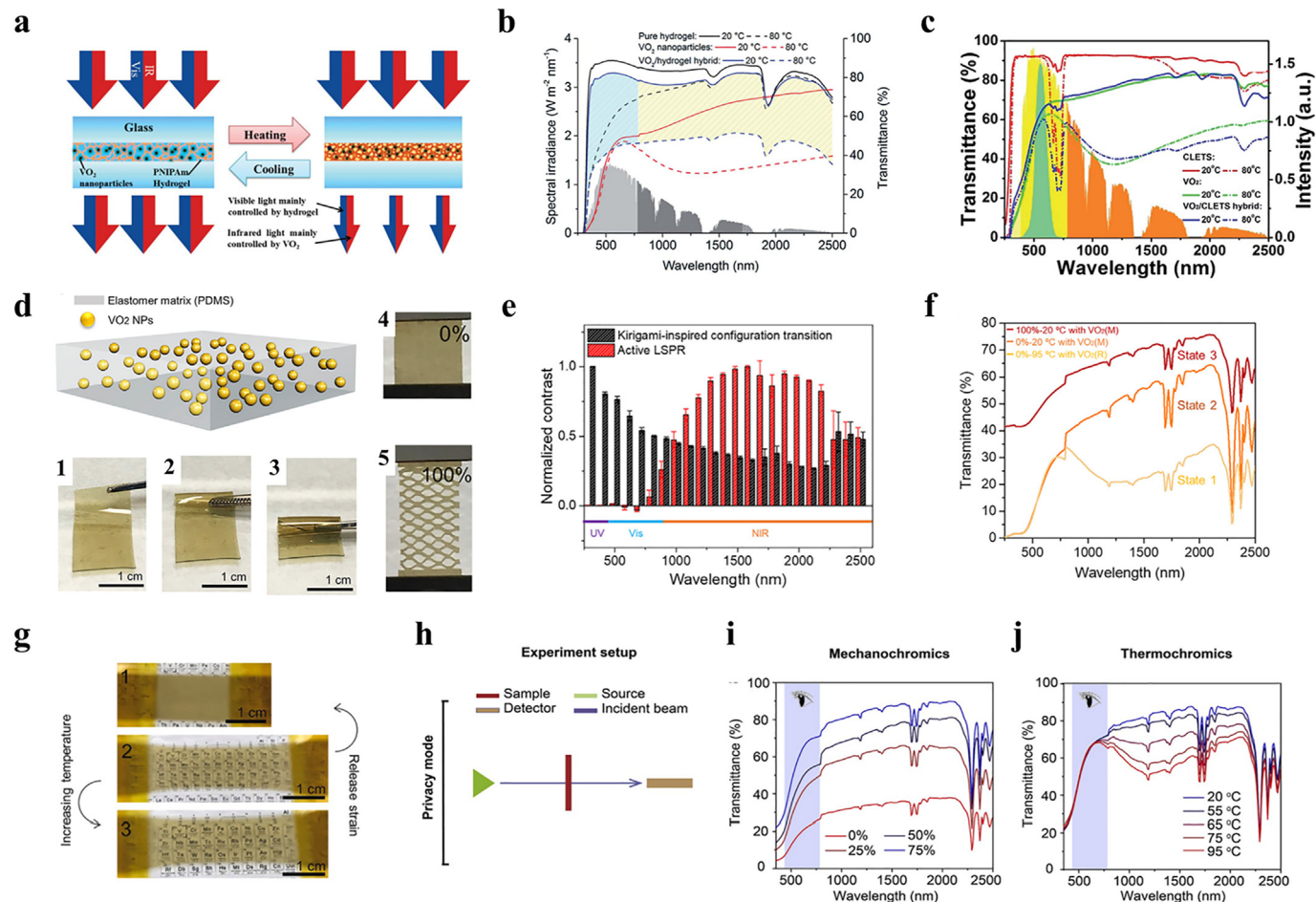


Fig. 9. Inorganic-organic hybrid coatings. (a) The schematic diagram of the VO₂/hydrogel hybrid coating and its solar modulation mechanism. (b) Transmittance spectra of pure hydrogel, VO₂ film, and VO₂/hydrogel film at 20 °C (solid lines) and 80 °C (dashed lines). The gray area refers to the solar spectral irradiance in the visible and near-infrared range. The luminous transmittance modulation of the VO₂/hydrogel film is colored with light cyan, and the near-infrared transmittance difference is covered with light yellow color. (c) Transmittance spectra of pure CLETS, VO₂ film, and VO₂/CLETS film at 20 °C (solid lines) and 80 °C (dashed lines). The yellow and orange areas represent the solar spectral irradiance in the visible and near-infrared range, respectively. The values of eye sensitivity function are denoted as the cyan area. (d) Scheme of VO₂-PDMS hybrid films. Photos of the synthesized yellowish VO₂-PDMS composite film in different rolled-up states are shown in d1-3. Kirigami VO₂-PDMS films under stretch (strain of 0% and 100%) in the parallel direction are illustrated in d4-5. (e) Normalized differences of solar transmittance in the visible and near-infrared range. (f) Transmittance spectra of the VO₂-PDMS composite film. States 1 and 2 refer to the kirigami VO₂-PDMS film with compact configuration at 90 °C and 20 °C, respectively. State 3 stands for the non-compact (strain of 100%) kirigami VO₂-PDMS film at 20 °C. (g) Photos of PVA/VO₂-PDMS films under (1) zero strain at 20 °C and 75% strain at (2) 20 °C and (3) 95 °C. (h-j) Privacy function mode of PVA/VO₂-PDMS structure: (h) the schematic diagram of the measurement setup to simulate the privacy mode, transmittance spectra of the film under (i) different strains and (j) temperatures. The figures were reproduced with the permissions from (a-b) Zhou et al. [108], Royal Society of Chemistry, (c) Zhu et al. [109], Royal Society of Chemistry, (d-f) Ke et al. [13], Elsevier, and (g-j) Ke et al. [112], Elsevier.

matrix, the VO₂ composite film exhibited superior flexibility and stretchability (Fig. 9d). An obvious increase of transmittance could be observed in the stretched kirigami VO₂-PDMS film because of the decrease of the effective areas while increasing strains. In the kirigami VO₂-PDMS film, two parts contributed to solar modulation efficiency across the MIT. One was the visible light modulation controlled by kirigami-induced configuration transition, and the other one was near-infrared modulation dominated by thermal-induced active LSPR (Fig. 9e). Both resulted in high ΔT_{sol} of up to 37.7% and enhanced T_{lum} (35.2%) in the stretched kirigami VO₂-PDMS film compared with the compact VO₂ film (Fig. 9f). Recently, their new design of the thermo-mechanochromic polyvinyl alcohol (PVA)-PDMS(VO₂) bilayer film [112] added privacy functionality to glass windows besides the energy-saving feature (Fig. 9g–j). This integration of both functions was achieved by regulating the scattering for privacy and absorbance in energy-saving modes.

Furthermore, organic polymers can introduce additional protections to VO₂ systems. A recent study showed that polydopamine, utilized as organic adhesive to the outside of VO₂@MgF₂, could improve its environmental durability by encapsulating the bulk defects [113]. More than 13 times enhancement of durability was observed when compared with a pristine VO₂ film.

Besides, the optical performance measurements of VO₂ coatings in most studies are based on the assumption that solar radiation is statically vertical, regardless of the impact of the solar elevation angle on the real energy-saving performance of VO₂ coatings. Long's group [114] fabricated a tilted one-dimensional grating-shape composite structure of polymer and VO₂/W-doped VO₂ nanoparticles on glass substrates via a three-dimensional printing technique and designed the tilted angle of the composite structure as per the actual solar elevation angle difference between summer and winter days. The grating structure exhibited angular selectivity in terms of angular and temporal characteristics [115]. A superior performance could be achieved for the tilted structure with 200 μm thickness, 200 μm spacing, and 200 μm width ($T_{\text{lum}} = 43.3\%$ and $\Delta T_{\text{sol}} = 25.8\%$). This new strategy for adaptive solar modulations provides more possibilities to improve TC performance.

4.3. Integration with the electrochromic device

Among different categories of smart windows, electrochromic (EC) and TC smart windows are promising for the practical applications in real life. In recent years, the integration of EC and TC materials for bifunctional smart windows has been proposed to accomplish adaptive regulation of the sunlight with simultaneously and independently responding to external stimuli such as electric stimulus and temperature change. This hybrid window commonly enables a combined modulation of visible light and near-infrared light.

Gao's group [116] reported the electrochromism-thermochromism dual response performance of the TiO₂(A)-VO₂ composite film (Fig. 10a). The optimized TiO₂-VO₂ film displayed good ΔT_{sol} (11.2%) with high T_{lum} (66.1% at 20 °C) across the temperature increment. In a dual-response mode (under an applied voltage of -5 V at 90 °C), an EC transmittance modulation at 630 nm (ΔT_{630}) of 19.1% was observed (Fig. 10b) accompanied with moderate T_{lum} of 44.7% and improved ΔT_{sol} of 17.1% (Fig. 10c). The amorphous WO₃ film was another effective EC material [117] and was used as the EC layer in the integrated structure to develop all-solid-state multifunctional smart windows (Fig. 10d) [118]. Four different optical states of the EC-TC hybrid were obtained as shown in Fig. 10e. After applying an input voltage of -2 V, the hybrid changed from the bleached state (bleached @RT) to the colored state (colored @RT). A further decrease in transmittance (Fig. 10f) occurred from the colored @RT state to colored @80 °C when the

temperature of the colored hybrid increased from the room temperature to 80 °C. Reversibly, the hybrid could recover to its original state after a reversed voltage of +2 V was applied, and the temperature of the hybrid returned to the room temperature. After this study, Jin's group [119] investigated the influence of EC layers on the TC behavior of VO₂ films in an all-solid-state EC-TC hybrid device. This hybrid device consisted of VO₂/LiTaO₃/WO₃ sandwiched structure (Fig. 10g) and demonstrated bifunctional EC-TC performance (Fig. 10h). Besides the four optical states reported in the former study, this multilayer device demonstrated a moderate T_{lum} (37.5%) and ultrahigh ΔT_{sol} (30.9%). The T_c of VO₂ decreased by more than 10 °C as a result of applied voltage, and the thermal hysteresis width of VO₂ became narrower because of Li⁺ insertion (Fig. 10i).

Besides the aforementioned methods to achieve the performance improvements, some real applications of VO₂-based smart windows are carried out. Gao et al. [120] examined the temperature difference between two houses (volume: 34 × 27 × 29 cm³) with and without VO₂ coatings posted on the glass window (25 × 30 cm²). They observed that the incorporation of the VO₂ coating could decrease the temperature of the house by 17 °C, reflecting the potential for energy-saving usage. Kim et al. [121] developed a versatile way to integrate VO₂ on flexible substrates in a large scale by using graphene as a platform. They further verified the solar irradiation blocking performance of the VO₂/graphene/PET film (12 × 12 cm²) using the similar way to Gao's experiment [120]. Zheng et al. [122] fabricated a large-scale TiO₂/VO₂/TiO₂ multilayer film with the area of 400 × 400 mm², which could reduce the temperature of the testing room by 12 °C under infrared irradiation. Ye et al. [123] built a testing room with the volume of 2.9 m × 1.8 m × 1.8 m and stuck the VO₂ film on the ordinary glass wall (1.65 m × 1.65 m) of the room. Their experiment showed that 10.2%–19.9% of cumulative cooling load could be saved for the room equipped with VO₂ glazing. Recently, Chen et al. [124] prepared VO₂ nanocrystal coating with a large size of 1.2 × 1.0 m² by a roll-coating method. Moreover, they analyzed the failure mechanism of VO₂ nanoparticles at the room temperature and improved the weatherability of VO₂ coatings with estimated usage life of 10 years (humidity: 60%).

The durability of VO₂ coatings should be enhanced because VO₂ is sensitive to oxygen and water in real environment and is likely to transform into other vanadium oxide phases. Protective structures, including core-shell structures (VO₂@ZnO [99]) and multilayer structure with encapsulated surfaces (VO₂/HfO₂ [125], Cr₂O₃/VO₂/SiO₂ [126]), are commonly used to inhibit the oxidation transformation and extend the service life of VO₂. For example, the service life of VO₂ could be extended up to 16 years because of the encapsulated layer of HfO₂ on VO₂ coating [125]. More recently, Long's group [127] fabricated a unique structure of the VO₂ nanocomposite film (VO₂ nanoparticles dispersed in the V₂O₅/V₃O₇ matrix) with a dense stable V₂O₅ overcoat. The V₂O₅ matrix and overcoat could protect the VO₂ film from degradation and enhance the T_{lum} and ΔT_{sol} because of the antireflection effect. Therefore, this VO₂ nanocomposite film could exhibit excellent TC performance ($T_{\text{lum}} = 42.2\%$ and $\Delta T_{\text{sol}} = 14.6\%$) for a remarkable service life of 23 years.

5. Summary and perspectives

In conclusion, VO₂-based TC films are intensively investigated for the application in smart windows. Most studies have focused on the modification of T_c and improvements of T_{lum} and ΔT_{sol} , which can be attributed to the passive response of VO₂ to ambient temperature. In this review, different methods such as doping and hybrid coatings have been summarized and discussed in detail. Moreover, electrothermal techniques which offer an alternative

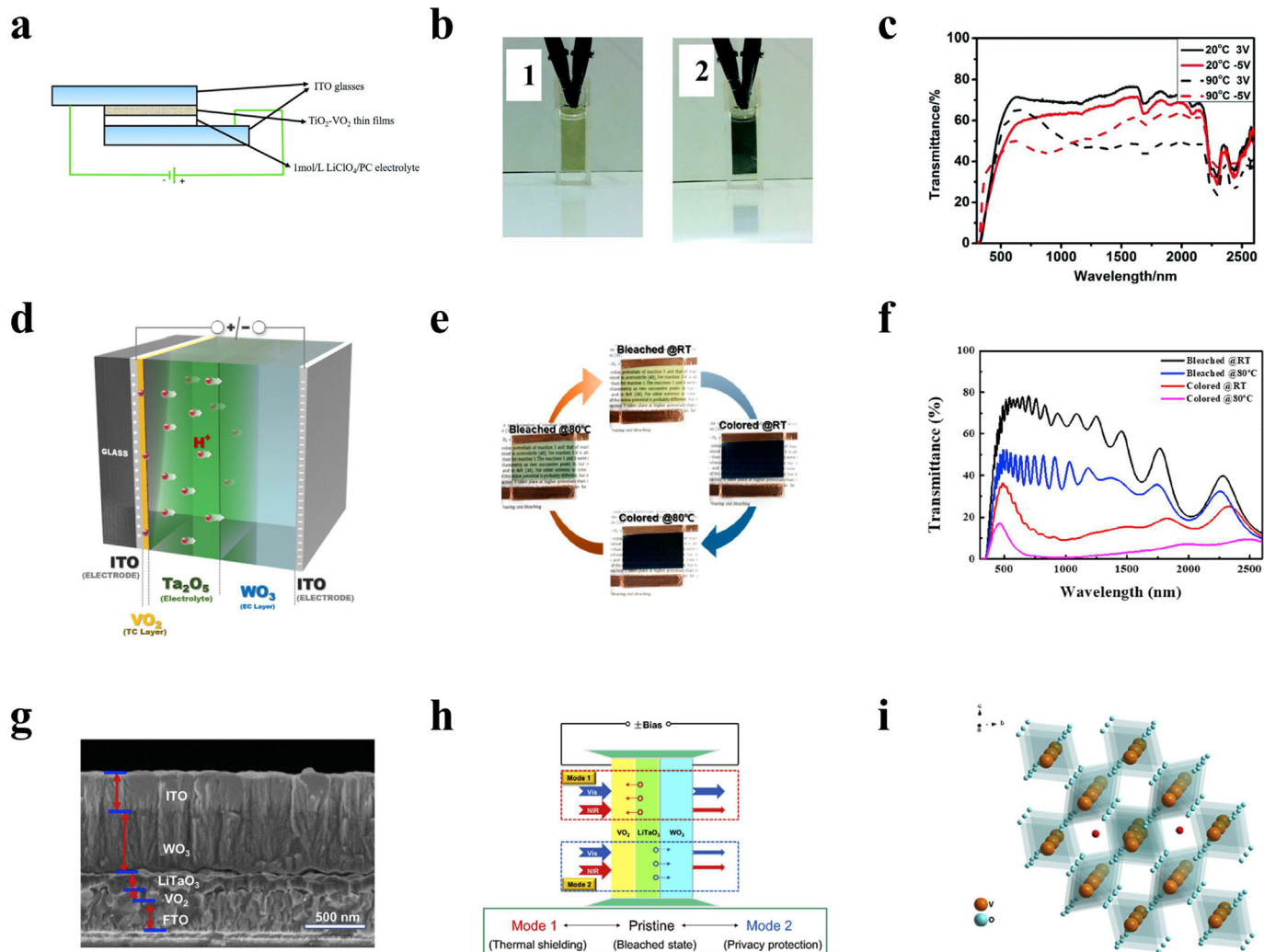


Fig. 10. Hybrid smart windows based on thermochromic VO_2 and electrochromic materials. (a) Scheme of the dual-response $\text{TiO}_2\text{-VO}_2$ device. (b) Photos of $\text{TiO}_2\text{-VO}_2$ films at bleached and colored states. (c) Transmittance spectra of the $\text{TiO}_2\text{-VO}_2$ device at varied temperature and applied voltages. (d) Schematic structure of the $\text{VO}_2\text{-WO}_3$ hybrid smart window. (e) Photos and (f) transmittance spectra of the $\text{VO}_2\text{-WO}_3$ hybrid device at four optical states. (g) Cross-sectional SEM of the five-layer structure of the $\text{VO}_2\text{-WO}_3$ hybrid device. (h) Scheme of the $\text{VO}_2\text{-WO}_3$ hybrid device in different functional modes. (i) Li^+ insertion within the VO_2 lattice driven by the applied electric field. The figures were reproduced with the permissions from (a–c) Yang et al. [116], Royal Society of Chemistry, (d–f) Lee et al. [118], American Chemical Society, and (g–i) Jia et al. [119], Elsevier.

way to control the MIT of VO_2 have been presented. The major progress of integrated hybrid structures with multifunctionalities has also been provided. There are yet important challenges and opportunities in the future of VO_2 -based smart windows, which are summarized as follows:

For the regulation of properties (including T_c , T_{lum} , and ΔT_{sol}) of VO_2 materials, currently it seems difficult for doped systems to achieve a superior performance for smart windows; therefore, more effective modulation strategies should be developed. As discussed in Section 4.2, inorganic-organic hybrids commonly demonstrate excellent optical properties as a result of the combined enhancement of visible and near-infrared modulation. Previous work on this type of hybrids concentrated on the incorporation of visible-regulating thermal responsive organic polymers. Thus, TC VO_2 combined with thermal-responsive polymers with the near-infrared regulating functionality would be a promising research direction for smart windows.

As for electrothermal techniques, different transparent conducting materials (ITO, FTO, AZO, etc.) have been reported as thermal conducting layers to heat up VO_2 , but the application of

electrically induced VO_2 in smart windows is just in its infancy, and series of problems need to be resolved. For instance, the criteria about the features of conducting material such as electric and thermal conductance values are still lacking. The feasibility of electrothermal technique on devices with small sizes (within square centimeter) has been verified by previous studies, but scale-up trials are seldom investigated. Besides, the selection of electrode material and the design of electrode structure are also important for the performance of VO_2 coatings.

Multifunctional coatings can be achieved by hybridizing with functional films such as photocatalytic and electrochromic materials. Focusing on the energy-saving performance of VO_2 -based smart windows, hybrids that can effectively enhance the near-infrared modulation ability or are easier for scalable applications should be developed. Certainly, there are some unexplored and efficient methods that can be utilized with thermochromism to accomplish high-performance, durable, and multifunctional smart windows. It is hoped that this review can map the progress to thrive the development of smart windows and bring new thoughts for future explorations in functional VO_2 -based devices.

Declaration of competing interest

The authors declare that they have no known competing financial interests or personal relationships that could have appeared to influence the work reported in this paper.

Acknowledgments

The authors acknowledge the support from Foundation of Shenzhen Science and Technology Innovation Committee (grant JCYJ20180302174026262), National Natural Science Foundation of China (grant 51776094, 91963129), Basic Research Project of Science and Technology of Shenzhen (grant JCYJ20180504165655180), and Foundation from Guangdong Provincial Key Laboratory of Energy Materials for Electric Power of Guangdong (grant 2018B030322001). This work is supported by Key Laboratory of Energy Conversion and Storage Technologies (Southern University of Science and Technology), Ministry of Education, the Shenzhen Engineering R&D Center for Flexible Solar Cells project funding from Shenzhen Development and Reform Committee (No. 2019-126), Student Innovation Training Program (grant nos. 2020X41 and 2020X42) from Southern University of Science and Technology (SUSTech), and the Special Funds for the Cultivation of Guangdong College Students' Scientific and Technological Innovation (pdjh2020c0008, pdjh2020c0009).

References

- [1] L.T. Kang, Y.F. Gao, H.J. Luo, A novel solution process for the synthesis of VO₂ thin films with excellent thermochromic properties, *ACS Appl. Mater. Interfaces* 1 (2009) 2211–2218, <https://doi.org/10.1021/am900375k>.
- [2] C. Wu, F. Feng, J. Feng, J. Dai, L. Peng, J. Zhao, J. Yang, C. Si, Z. Wu, Y. Xie, Hydrogen-incorporation stabilization of metallic VO₂ (R) phase to room temperature, displaying promising low-temperature thermoelectric effect, *J. Am. Chem. Soc.* 133 (2011) 13798–13801, <https://doi.org/10.1021/ja203186f>.
- [3] A. Zylibersztein, Metal-insulator transition in vanadium dioxide, *Phys. Rev. B* 11 (1975) 4383–4395, <https://doi.org/10.1103/PhysRevB.11.4383>.
- [4] N. Shen, B. Dong, C. Cao, Z. Chen, H. Luo, Y. Gao, Solid-state-reaction synthesis of VO₂ nanoparticles with low phase transition temperature, enhanced chemical stability and excellent thermochromic properties, *RSC Adv.* 5 (2015) 108015–108022, <https://doi.org/10.1039/c5ra20732k>.
- [5] X. Qian, N. Wang, Y. Li, J. Zhang, Z. Xu, Y. Long, Bioinspired multifunctional vanadium dioxide: improved thermochromism and hydrophobicity, *Langmuir* 30 (2014) 10766–10771, <https://doi.org/10.1021/la502787q>.
- [6] C.S. Blackman, C. Piccirillo, R. Binions, I.P. Parkin, Atmospheric pressure chemical vapour deposition of thermochromic tungsten doped vanadium dioxide thin films for use in architectural glazing, *Thin Solid Films* 517 (2009) 4565–4570, <https://doi.org/10.1016/j.tsf.2008.12.050>.
- [7] I.P. Parkin, T.D. Manning, Intelligent thermochromic windows, *J. Chem. Educ.* 83 (2006) 393, <https://doi.org/10.1021/ed083p393>.
- [8] S.Y. Li, G.A. Niklasson, C.G. Granqvist, Thermochromic fenestration with VO₂-based materials: three challenges and how they can be met, *Thin Solid Films* 520 (2012) 3823–3828, <https://doi.org/10.1016/j.tsf.2011.10.053>.
- [9] Y. Cui, Y. Ke, C. Liu, Z. Chen, N. Wang, L. Zhang, Y. Zhou, S. Wang, Y. Gao, Y. Long, Thermochromic VO₂ for energy-efficient smart windows, *Joule* 2 (2018) 1707–1746, <https://doi.org/10.1016/j.joule.2018.06.018>.
- [10] Y. Ke, C. Zhou, Y. Zhou, S. Wang, S.H. Chan, Y. Long, Emerging thermal-responsive materials and integrated techniques targeting the energy-efficient smart window application, *Adv. Funct. Mater.* 28 (2018), <https://doi.org/10.1002/adfm.201800113>.
- [11] R. Shi, N. Shen, J. Wang, W. Wang, A. Amini, N. Wang, C. Cheng, Recent advances in fabrication strategies, phase transition modulation, and advanced applications of vanadium dioxide, *Appl. Phys. Rev.* 6 (2019), 011312, <https://doi.org/10.1063/1.5087864>.
- [12] X. Cao, T. Chang, Z. Shao, F. Xu, H. Luo, P. Jin, Challenges and opportunities toward real application of VO₂-based smart glazing, *Matter* 2 (2020) 862–881, <https://doi.org/10.1016/j.matt.2020.02.009>.
- [13] Y. Ke, Y. Yin, Q. Zhang, Y. Tan, P. Hu, S. Wang, Y. Tang, Y. Zhou, X. Wen, S. Wu, T.J. White, J. Yin, J. Peng, Q. Xiong, D. Zhao, Y. Long, Adaptive thermochromic windows from active plasmonic elastomers, *Joule* 3 (2019) 858–871, <https://doi.org/10.1016/j.joule.2018.12.024>.
- [14] Z. Chen, Y. Gao, L. Kang, C. Cao, S. Chen, H. Luo, Fine crystalline VO₂ nanoparticles: synthesis, abnormal phase transition temperatures and excellent optical properties of a derived VO₂ nanocomposite foil, *J. Mater. Chem. A* 2 (2014) 2718–2727, <https://doi.org/10.1039/c3ta14612j>.
- [15] J.D. Budai, J. Hong, M.E. Manley, E.D. Specht, C.W. Li, J.Z. Tischler, D.L. Abernathy, A.H. Said, B.M. Leu, L.A. Boatner, R.J. McQueeney, O. Delaire, Metallization of vanadium dioxide driven by large phonon entropy, *Nature* 515 (2014) 535–539, <https://doi.org/10.1038/nature13865>.
- [16] Y. Gao, S. Wang, H. Luo, L. Dai, C. Cao, Y. Liu, Z. Chen, M. Kanehira, Enhanced chemical stability of VO₂ nanoparticles by the formation of SiO₂/VO₂ core/shell structures and the application to transparent and flexible VO₂-based composite foils with excellent thermochromic properties for solar heat control, *Energy Environ. Sci.* 5 (2012) 6104–6110, <https://doi.org/10.1039/c2ee02803d>.
- [17] M. Netsianda, P.E. Ngoepe, C. Richard, A. Catlow, S.M. Woodley, The displacive phase transition of vanadium dioxide and the effect of doping with tungsten, *Chem. Mater.* 20 (2008) 1764–1772, <https://doi.org/10.1021/cm701861z>.
- [18] L. Whittaker, C. Jaye, Z.G. Fu, D.A. Fischer, S. Banerjee, Depressed phase transition in solution-grown VO₂ nanostructures, *J. Am. Chem. Soc.* 131 (2009) 8884–8894, <https://doi.org/10.1021/ja902054w>.
- [19] K. Shibuya, M. Kawasaki, Y. Tokura, Metal-insulator transition in epitaxial V_{1-x}W_xO₂ (0 < x < 0.33) thin films, *Appl. Phys. Lett.* 96 (2010), 022102, <https://doi.org/10.1039/c13291053>.
- [20] Y.F. Zhang, W. Li, M.J. Fan, F.F. Zhang, J.C. Zhang, X.H. Liu, H.N. Zhang, C. Huang, H.B. Li, Preparation of W- and Mo-doped VO₂ (M) by ethanol reduction of peroxovanadium complexes and their phase transition and optical switching properties, *J. Alloys Compd.* 544 (2012) 30–36, <https://doi.org/10.1016/j.jallcom.2012.07.093>.
- [21] D. Li, M. Li, J. Pan, Y. Luo, H. Wu, Y. Zhang, G. Li, Hydrothermal synthesis of Mo-doped VO₂/TiO₂ composite nanocrystals with enhanced thermochromic performance, *ACS Appl. Mater. Interfaces* 6 (2014) 6555–6561, <https://doi.org/10.1021/am500135d>.
- [22] C. Batista, J. Carneiro, R.M. Ribeiro, V. Teixeira, Reactive pulsed-DC sputtered Nb-doped VO₂ coatings for smart thermochromic windows with active solar control, *J. Nanosci. Nanotechnol.* 11 (2011) 9042–9045, <https://doi.org/10.1166/jnn.2011.3486>.
- [23] S. Guan, M. Souquet-Basiége, O. Toulemonde, D. Denoux, N. Penin, M. Gaudon, A. Rougier, Toward room-temperature thermochromism of VO₂ by Nb doping: magnetic investigations, *Chem. Mater.* 31 (2019) 9819–9830, <https://doi.org/10.1021/acs.chemmater.9b03906>.
- [24] H.-Y. Lee, C.-L. Wu, C.-H. Kao, C.-T. Lee, S.-F. Tang, W.-J. Lin, H.-C. Chen, J.-C. Lin, Investigated performance of uncooled tantalum-doped VO_x floating-type microbolometers, *Appl. Surf. Sci.* 354 (2015) 106–109, <https://doi.org/10.1016/j.apsusc.2015.03.008>.
- [25] S. Chen, Z. Wang, H. Ren, Y. Chen, W. Yan, C. Wang, B. Li, J. Jiang, C. Zou, Gate-controlled VO₂ phase transition for high-performance smart windows, *Sci. Adv.* 5 (2019), [https://doi.org/10.1126/sciadv.aav6815 eaav6815](https://doi.org/10.1126/sciadv.aav6815).
- [26] R. Shi, J. Wang, X. Cai, L. Zhang, P. Chen, S. Liu, L. Zhang, W. Ouyang, N. Wang, C. Cheng, Axial modulation of metal-insulator phase transition of VO₂ nanowires by graded doping engineering for optically readable thermometers, *J. Phys. Chem. C* 121 (2017) 24877–24885, <https://doi.org/10.1021/acs.jpcc.7b08946>.
- [27] Z. Zou, Z. Zhang, J. Xu, Z. Yu, M. Cheng, R. Xiong, Z. Lu, Y. Liu, J. Shi, Thermochromic, threshold switching, and optical properties of Cr-doped VO₂ thin films, *J. Alloys Compd.* 806 (2019) 310–315, <https://doi.org/10.1016/j.jallcom.2019.07.264>.
- [28] A.O. Suleiman, S. Mansouri, N. Emond, B. Le Drogoff, T. Begin, J. Margot, M. Chaker, Probing the role of thermal vibrational disorder in the SPT of VO₂ by Raman spectroscopy, *Sci. Rep.* 11 (2021) 1620, <https://doi.org/10.1038/s41598-020-79758-1>.
- [29] S. Guan, M. Gaudon, M. Souquet-Basiége, O. Viraphong, N. Penin, A. Rougier, Carbon-reduction as an easy route for the synthesis of VO₂ (M1) and further Al, Ti doping, *Dalton Trans.* 48 (2019) 3080–3089, <https://doi.org/10.1039/c8dt04914a>.
- [30] H. Zhu, Z. Zhang, X. Jiang, Effect of Al, Ti and Cr doping on vanadium dioxide (VO₂) analyzed by density function theory (DFT) method, *J. Nanosci. Nanotechnol.* 20 (2020) 1651–1659, <https://doi.org/10.1166/jnn.2020.17140>.
- [31] R. Chen, L. Miao, h. cheng, N. Eiji, C. Liu, A. Toru, Y. Iwamoto, M. Takata, S. Tanemura, One-step hydrothermal synthesis of V_{1-x}W_xO₂ (M/R) nanorods with superior doping efficiency and thermochromic property, *J. Mater. Chem. A* 3 (2015) 3726–3738, <https://doi.org/10.1039/c4ta05559d>.
- [32] N. Shen, B. Dong, C. Cao, Z. Chen, J. Liu, H. Luo, Y. Gao, Lowered phase transition temperature and excellent solar heat shielding properties of well-crystallized VO₂ by W doping, *Phys. Chem. Chem. Phys.* 18 (2016) 28010–28017, <https://doi.org/10.1039/c6cp05143j>.
- [33] L. Zhang, F. Xia, J. Yao, T. Zhu, H. Xia, G. Yang, B. Liu, Y. Gao, Facile synthesis, formation mechanism and thermochromic properties of W-doped VO₂ (M) nanoparticles for smart window applications, *J. Mater. Chem. C* 8 (2020) 13396–13404, <https://doi.org/10.1039/d0tc03436c>.
- [34] C.L. Gomez-Heredia, J.A. Ramirez-Rincon, D. Bhardwaj, P. Rajasekar, I.J. Tadeo, J.L. Cervantes-Lopez, J. Ordóñez-Miranda, O. Ares, A.M. Umarji, J. Drevillon, K. Joulain, Y. Ezzahri, J.J. Alvarado-Gil, Measurement of the hysteretic thermal properties of W-doped and undoped nanocrystalline powders of VO₂, *Sci. Rep.* 9 (2019) 14687, <https://doi.org/10.1038/s41598-019-51162-4>.
- [35] A.E. Ersundu, M. Çelikbilek Ersundu, E. Doğan, M.B. Güven, A comparative investigation on thermal, structural and optical properties of W and Nb-

- doped VO₂-based thermochromic thin films, *Thin Solid Films* 700 (2020) 137919, <https://doi.org/10.1016/j.tsf.2020.137919>.
- [36] D.G. Sellers, E.J. Braham, R. Villarreal, B. Zhang, A. Parija, T.D. Brown, T.E.G. Alivio, H. Clarke, L.R. De Jesus, L. Zuin, D. Prendergast, X. Qian, R. Arroyave, P.J. Shamberger, S. Banerjee, Atomic hourglass and thermometer based on diffusion of a mobile dopant in VO₂, *J. Am. Chem. Soc.* 142 (2020) 15513–15526, <https://doi.org/10.1021/jacs.0c07152>.
- [37] J.J. Zhang, H.Y. He, Y. Xie, B.C. Pan, Boron-tuning transition temperature of vanadium dioxide from rutile to monoclinic phase, *J. Chem. Phys.* 141 (2014) 194707, <https://doi.org/10.1063/1.4901514>.
- [38] T.E.G. Alivio, D.G. Sellers, H. Asayesh-Ardakani, E.J. Braham, G.A. Horrocks, K.E. Pelcher, R. Villareal, L. Zuin, P.J. Shamberger, R. Arroyave, R. Shahbazian-Yassar, S. Banerjee, Postsynthetic route for modifying the metal–insulator transition of VO₂ by interstitial dopant incorporation, *Chem. Mater.* 29 (2017) 5401–5412, <https://doi.org/10.1021/acs.chemmater.7b02029>.
- [39] A. Yano, H. Clarke, D.G. Sellers, E.J. Braham, T.E.G. Alivio, S. Banerjee, P.J. Shamberger, Toward high-precision control of transformation characteristics in VO₂ through dopant modulation of hysteresis, *J. Phys. Chem. C* 124 (2020) 21223–21231, <https://doi.org/10.1021/acs.jpcc.0c04952>.
- [40] T. Hajlaoui, N. Émond, C. Quiroquette, B. Le Drogoff, J. Margot, M. Chaker, Metal–insulator transition temperature of boron-doped VO₂ thin films grown by reactive pulsed laser deposition, *Scripta Mater.* 177 (2020) 32–37, <https://doi.org/10.1016/j.scriptamat.2019.09.019>.
- [41] Q. Zhou, W. Lv, Q. Qiu, T. Zhou, C. Huang, L. Li, Boron doped M-phase VO₂ nanoparticles with low metal-insulator phase transition temperature for smart windows, *Ceram. Int.* 46 (2020) 4786–4794, <https://doi.org/10.1016/j.ceramint.2019.10.211>.
- [42] N.R. Mlyuka, G.A. Niklasson, C.G. Granqvist, Mg doping of thermochromic VO₂ films enhances the optical transmittance and decreases the metal–insulator transition temperature, *Appl. Phys. Lett.* 95 (2009) 171909, <https://doi.org/10.1063/1.3229949>.
- [43] S.L. Hu, S.Y. Li, R. Ahuja, C.G. Granqvist, K. Hermansson, G.A. Niklasson, R.H. Scheicher, Optical properties of Mg-doped VO₂: absorption measurements and hybrid functional calculations, *Appl. Phys. Lett.* 101 (2012) 201902, <https://doi.org/10.1063/1.4766167>.
- [44] S.-Y. Li, N.R. Mlyuka, D. Premetzhofer, A. Hallén, G.r. Possnert, G.A. Niklasson, C.G. Granqvist, Bandgap widening in thermochromic Mg-doped VO₂ thin films: quantitative data based on optical absorption, *Appl. Phys. Lett.* 103 (2013) 161907, <https://doi.org/10.1063/1.4826444>.
- [45] J.D. Zhou, Y.F. Gao, X.L. Liu, Z. Chen, L. Dai, C.X. Cao, H.J. Luo, M. Kanahira, C. Sun, L.M. Yan, Mg-doped VO₂ nanoparticles: hydrothermal synthesis, enhanced visible transmittance and decreased metal-insulator transition temperature, *Phys. Chem. Chem. Phys.* 15 (2013) 7505–7511, <https://doi.org/10.1039/c3cp50638j>.
- [46] M. Panagopoulou, E. Gagaoudakis, N. Boukos, E. Aperathitis, G. Kiriakidis, D. Tsoukalas, Y.S. Raptis, Thermochromic performance of Mg-doped VO₂ thin films on functional substrates for glazing applications, *Sol. Energy Mater. Sol. Cells* 157 (2016) 1004–1010, <https://doi.org/10.1016/j.solmat.2016.08.021>.
- [47] Z. Wen, Y. Ke, C. Feng, S. Fang, M. Sun, X. Liu, Y. Long, Mg-doped VO₂/ZrO₂ core-shell nanoflakes for thermochromic smart windows with enhanced performance, *Adv. Mater. Interfaces* 8 (2021) 2001606, <https://doi.org/10.1002/admi.202001606>.
- [48] S. Chen, L. Dai, J. Liu, Y. Gao, X. Liu, Z. Chen, J. Zhou, C. Cao, P. Han, H. Luo, M. Kanahira, The visible transmittance and solar modulation ability of VO₂ flexible foils simultaneously improved by Ti doping: an optimization and first principle study, *Phys. Chem. Chem. Phys.* 15 (2013) 17537–17543, <https://doi.org/10.1039/c3cp52009a>.
- [49] N. Shen, S. Chen, Z. Chen, X. Liu, C. Cao, B. Dong, H. Luo, J. Liu, Y. Gao, The synthesis and performance of Zr-doped and W–Zr-codoped VO₂ nanoparticles and derived flexible foils, *J. Mater. Chem. A* 2 (2014) 15087–15093, <https://doi.org/10.1039/c4ta02880e>.
- [50] P. Kiri, M.E.A. Warwick, I. Ridley, R. Binions, Fluorine doped vanadium dioxide thin films for smart windows, *Thin Solid Films* 520 (2011) 1363–1366, <https://doi.org/10.1016/j.tsf.2011.01.401>.
- [51] W. Burkhardt, T. Christmann, S. Franke, W. Kriegseis, D. Meister, B.K. Meyer, W. Niessner, D. Schalch, A. Scharmann, Tungsten and fluorine co-doping of VO₂ films, *Thin Solid Films* 402 (2002) 226–231, [https://doi.org/10.1016/S0040-6090\(01\)01603-0](https://doi.org/10.1016/S0040-6090(01)01603-0).
- [52] L. Dai, S. Chen, J. Liu, Y. Gao, J. Zhou, Z. Chen, C. Cao, H. Luo, M. Kanahira, F-doped VO₂ nanoparticles for thermochromic energy-saving foils with modified color and enhanced solar-heat shielding ability, *Phys. Chem. Chem. Phys.* 15 (2013) 11723–11729, <https://doi.org/10.1039/c3cp51359a>.
- [53] I. Abdellaoui, G. Merad, M. Maaza, H.S. Abdelkader, Electronic and optical properties of Mg-, F-doped and Mg/F-codoped M1-VO₂ via hybrid density functional calculations, *J. Alloys Compd.* 658 (2016) 569–575, <https://doi.org/10.1016/j.jallcom.2015.10.248>.
- [54] A. Riapanitra, Y. Asakura, W. Cao, Y. Noda, S. Yin, Supercritical temperature synthesis of fluorine-doped VO₂ (M) nanoparticle with improved thermochromic property, *Nanotechnology* 29 (2018) 244005, <https://doi.org/10.1088/1361-6528/aa8752>.
- [55] Z. Zhao, Y. Liu, Z. Yu, C. Ling, J. Li, Y. Zhao, H. Jin, Sn–W Co-doping improves thermochromic performance of VO₂ films for smart windows, *ACS Appl. Energy Mater.* 3 (2020) 9972–9979, <https://doi.org/10.1021/acs.ame.0c01651>.
- [56] N. Wang, S. Liu, X.T. Zeng, S. Magdassi, Y. Long, Mg/W-codoped vanadium dioxide thin films with enhanced visible transmittance and low phase transition temperature, *J. Mater. Chem. C* 3 (2015) 6771–6777, <https://doi.org/10.1039/c5tc01062d>.
- [57] M.K. Dietrich, F. Kuhl, A. Polity, P.J. Klar, Optimizing thermochromic VO₂ by co-doping with W and Sr for smart window applications, *Appl. Phys. Lett.* 110 (2017) 141907, <https://doi.org/10.1063/1.4979700>.
- [58] C. Ji, Z. Wu, L. Lu, X. Wu, J. Wang, X. Liu, H. Zhou, Z. Huang, J. Gou, Y. Jiang, High thermochromic performance of Fe/Mg co-doped VO₂ thin films for smart window applications, *J. Mater. Chem. C* 6 (2018) 6502–6509, <https://doi.org/10.1039/c8tc01111g>.
- [59] J. Yan, Y. Zhang, W. Huang, M. Tu, Effect of Mo–W Co-doping on semiconductor-metal phase transition temperature of vanadium dioxide film, *Thin Solid Films* 516 (2008) 8554–8558, <https://doi.org/10.1016/j.tsf.2008.05.021>.
- [60] Y. Xu, W. Huang, Q. Shi, Y. Zhang, L. Song, Y. Zhang, Synthesis and properties of Mo and W ions co-doped porous nano-structured VO₂ films by sol-gel process, *J. Sol. Gel Sci. Technol.* 64 (2012) 493–499, <https://doi.org/10.1007/s10971-012-2881-9>.
- [61] H.J. Kim, D.K. Roh, J.W. Yoo, D.-S. Kim, Designable phase transition temperature of VO₂ Co-doped with Nb and W elements for smart window application, *J. Nanosci. Nanotechnol.* 19 (2019) 7185–7191, <https://doi.org/10.1166/jnn.2019.16618>.
- [62] W. Lv, D. Huang, Y. Chen, Q. Qiu, Z. Luo, Synthesis and characterization of Mo–W co-doped VO₂ (R) nano-powders by the microwave-assisted hydrothermal method, *Ceram. Int.* 40 (2014) 12661–12668, <https://doi.org/10.1016/j.ceramint.2014.04.113>.
- [63] S.H. Bae, S. Lee, H. Koo, L. Lin, B.H. Jo, C. Park, Z.L. Wang, The memristive properties of a single VO₂ nanowire with switching controlled by self-heating, *Adv. Mater.* 25 (2013) 5098–5103, <https://doi.org/10.1002/adma.201302511>.
- [64] A. Zimmers, L. Aigouy, M. Mortier, A. Sharoni, S. Wang, K.G. West, J.G. Ramirez, I.K. Schuller, Role of thermal heating on the voltage induced insulator–metal transition in VO₂, *Phys. Rev. Lett.* 110 (2013), 056601, <https://doi.org/10.1103/PhysRevLett.110.056601>.
- [65] I.P. Radu, B. Govoreanu, S. Mertens, X. Shi, M. Cantoro, M. Schaekers, M. Jurczak, S. De Gendt, A. Stesmans, J.A. Kittl, M. Heyns, K. Martens, Switching mechanism in two-terminal vanadium dioxide devices, *Nanotechnology* 26 (2015) 165202, <https://doi.org/10.1088/0957-4484/26/16/165202>.
- [66] J. Yoon, G. Lee, C. Park, B.S. Mun, H. Ju, Investigation of length-dependent characteristics of the voltage-induced metal insulator transition in VO₂ film devices, *Appl. Phys. Lett.* 105 (2014), 083503, <https://doi.org/10.1063/1.4893783>.
- [67] M. Farjadian, M. Shalchian, Hybrid electrothermal model for insulator-to-metal transition in VO₂ thin films, *IEEE Trans. Electron. Dev.* 68 (2021) 704–712, <https://doi.org/10.1109/ted.2020.3043208>.
- [68] G.M. Liao, S. Chen, L.L. Fan, Y.L. Chen, X.Q. Wang, H. Ren, Z.M. Zhang, C.W. Zou, Dynamically tracking the joule heating effect on the voltage induced metal–insulator transition in VO₂ crystal film, *AIP Adv.* 6 (2016), 045014, <https://doi.org/10.1063/1.4948311>.
- [69] M. Li, S. Ji, J. Pan, H. Wu, L. Zhong, Q. Wang, F. Li, G. Li, Infrared response of self-heating VO₂ nanoparticles film based on Ag nanowires heater, *J. Mater. Chem. A* 2 (2014) 20470–20473, <https://doi.org/10.1039/C4TA04738A>.
- [70] M. Li, H. Wu, L. Zhong, H. Wang, Y. Luo, G. Li, Active and dynamic infrared switching of VO₂ (M) nanoparticle film on ITO glass, *J. Mater. Chem. C* 4 (2016) 1692–1703, <https://doi.org/10.1039/c5tc04039f>.
- [71] R. Hao, Y. Li, F. Liu, Y. Sun, J. Tang, P. Chen, W. Jiang, Z. Wu, T. Xu, B. Fang, Electric field induced metal–insulator transition in VO₂ thin film based on FTO/VO₂/FTO structure, *Infrared Phys. Technol.* 75 (2016) 82–86, <https://doi.org/10.1016/j.infrared.2015.12.012>.
- [72] Z. Xu, G. Qin, A.A. Bernussi, Z. Fan, Electrothermally control of dynamic infrared switching of VO₂ thin film on FTO glass, *J. Alloys Compd.* 858 (2021) 157640, <https://doi.org/10.1016/j.jallcom.2020.157640>.
- [73] L. Fan, Y. Chen, Q. Liu, S. Chen, L. Zhu, Q. Meng, B. Wang, Q. Zhang, H. Ren, C. Zou, Infrared response and optoelectronic memory device fabrication based on epitaxial VO₂ film, *ACS Appl. Mater. Interfaces* 8 (2016) 32971–32977, <https://doi.org/10.1021/acsm.6b12831>.
- [74] J.R. Skusa, D.W. Scott, R.M. Mundle, A.K. Pradhan, Electro-thermal control of aluminum-doped zinc oxide/vanadium dioxide multilayered thin films for smart-device applications, *Sci. Rep.* 6 (2016) 21040, <https://doi.org/10.1038/srep21040>.
- [75] P. Zhang, W. Zhang, J. Wang, K. Jiang, J. Zhang, W. Li, J. Wu, Z. Hu, J. Chu, The electro-optic mechanism and infrared switching dynamic of the hybrid multilayer VO₂/Al:ZnO heterojunctions, *Sci. Rep.* 7 (2017) 4425, <https://doi.org/10.1038/s41598-017-04660-2>.
- [76] H. Xiao, Y. Li, B. Fang, X. Wang, Z. Liu, J. Zhang, Z. Li, Y. Huang, J. Pei, Voltage-induced switching dynamics based on an AZO/VO₂/AZO sandwiched structure, *Infrared Phys. Technol.* 86 (2017) 212–217, <https://doi.org/10.1016/j.infrared.2017.09.010>.
- [77] H. Zhang, Z. Wu, C. Wang, Y. Sun, VO₂ film with small hysteresis width and low transition temperature, *Vacuum* 170 (2019) 108971, <https://doi.org/10.1016/j.vacuum.2019.108971>.
- [78] Y. Chen, L. Fan, Q. Fang, W. Xu, S. Chen, G. Zan, H. Ren, L. Song, C. Zou, Free-standing SWNTs/VO₂/Mica hierarchical films for high-performance thermochromic devices, *Nano Energy* 31 (2017) 144–151, <https://doi.org/10.1016/j.nanoen.2016.11.030>.

- [79] N. Shen, S. Chen, W. Wang, R. Shi, P. Chen, D. Kong, Y. Liang, A. Amini, J. Wang, C. Cheng, Joule heating driven infrared switching in flexible VO₂ nanoparticle films with reduced energy consumption for smart windows, *J. Mater. Chem. A* 7 (2019) 4516–4524, <https://doi.org/10.1039/c8ta11071a>.
- [80] Q. Hao, W. Li, H. Xu, J. Wang, Y. Yin, H. Wang, L. Ma, F. Ma, X. Jiang, O.G. Schmidt, P.K. Chu, VO₂/TiN plasmonic thermochromic smart coatings for room-temperature applications, *Adv. Mater.* 30 (2018) 1705421, <https://doi.org/10.1002/adma.201705421>.
- [81] X. Zhou, TiO₂-Supported single-atom catalysts for photocatalytic reactions, *Acta Phys. Chim. Sin.* 37 (2020) 2008064, <https://doi.org/10.3866/pku.Whxb202008064>.
- [82] J. Li, X. Wu, S. Liu, Fluorinated TiO₂ hollow photocatalysts for photocatalytic applications, *Acta Phys. Chim. Sin.* 37 (2020) 2009038, <https://doi.org/10.3866/pku.Whxb202009038>.
- [83] M.J. Powell, R. Quesada-Cabrera, A. Taylor, D. Teixeira, I. Papakonstantinou, R.G. Palgrave, G. Sankar, I.P. Parkin, Intelligent multifunctional VO₂/SiO₂/TiO₂ coatings for self-cleaning, energy-saving window panels, *Chem. Mater.* 28 (2016) 1369–1376, <https://doi.org/10.1021/acs.chemmater.5b04419>.
- [84] N.R. Mlyuka, G.A. Niklasson, C.G. Granqvist, Thermochromic multilayer films of VO₂ and TiO₂ with enhanced transmittance, *Sol. Energy Mater. Sol. Cells* 93 (2009) 1685–1687, <https://doi.org/10.1016/j.solmat.2009.03.021>.
- [85] Z. Chen, Y. Gao, L. Kang, J. Du, Z. Zhang, H. Luo, H. Miao, G. Tan, VO₂-based double-layered films for smart windows: optical design, all-solution preparation and improved properties, *Sol. Energy Mater. Sol. Cells* 95 (2011) 2677–2684, <https://doi.org/10.1016/j.solmat.2011.05.041>.
- [86] I. Top, R. Binions, M.E.A. Warwick, C.W. Dunnill, M. Holdynski, I. Abrahams, VO₂/TiO₂ bilayer films for energy efficient windows with multifunctional properties, *J. Mater. Chem. C* 6 (2018) 4485–4493, <https://doi.org/10.1039/c8tc00835c>.
- [87] Y. Ji, A. Mattsson, G.A. Niklasson, C.G. Granqvist, L. Österlund, Synergistic TiO₂/VO₂ window coating with thermochromism, enhanced luminous transmittance, and photocatalytic activity, *Joule* 3 (2019) 2457–2471, <https://doi.org/10.1016/j.joule.2019.06.024>.
- [88] S. Liu, C.Y. Tso, H.H. Lee, Y. Zhang, K.M. Yu, C.Y.H. Chao, Bio-inspired TiO₂ nano-cone antireflection layer for the optical performance improvement of VO₂ thermochromic smart windows, *Sci. Rep.* 10 (2020) 11376, <https://doi.org/10.1038/s41598-020-68411-6>.
- [89] T.D. Vu, X. Cao, H. Hu, J. Bao, T. Cao, J. Hu, X. Zeng, Y. Long, A universal robust bottom-up approach to engineer Greta-oto-inspired anti-reflective structure, *Cell Rep. Phys. Sci.* 2 (2021) 100479, <https://doi.org/10.1016/j.jcrp.2021.100479>.
- [90] S.T. Li, Y.M. Li, M. Jiang, S.D. Ji, H.J. Luo, Y.F. Gao, P. Jin, Preparation and characterization of self-supporting thermochromic films composed of VO₂(M)@SiO₂ nanofibers, *ACS Appl. Mater. Interfaces* 5 (2013) 6453–6457, <https://doi.org/10.1021/am401839d>.
- [91] L. Zhao, L. Miao, C. Liu, C. Li, T. Asaka, Y. Kang, Y. Iwamoto, S. Tanemura, H. Gu, H. Su, Solution-processed VO₂-SiO₂ composite films with simultaneously enhanced luminous transmittance, solar modulation ability and anti-oxidation property, *Sci. Rep.* 4 (2014) 7000, <https://doi.org/10.1038/srep07000>.
- [92] J. Zhang, J. Wang, C. Yang, H. Jia, X. Cui, S. Zhao, Y. Xu, Mesoporous SiO₂/VO₂ double-layer thermochromic coating with improved visible transmittance for smart window, *Sol. Energy Mater. Sol. Cells* 162 (2017) 134–141, <https://doi.org/10.1016/j.solmat.2016.12.048>.
- [93] X. Lu, X. Xiao, Z. Cao, Y. Zhan, H. Cheng, G. Xu, A novel method to modify the color of VO₂-based thermochromic smart films by solution-processed VO₂@SiO₂@Au core–shell nanoparticles, *RSC Adv.* 6 (2016) 47249–47257, <https://doi.org/10.1039/c6ra07594k>.
- [94] S.Y. Li, G.A. Niklasson, C.G. Granqvist, Nanothermochromics: calculations for VO₂ nanoparticles in dielectric hosts show much improved luminous transmittance and solar energy transmittance modulation, *J. Appl. Phys.* 108 (2010), <https://doi.org/10.1063/1.3487980>.
- [95] M. Wang, J. Tian, H. Zhang, X. Shi, Z. Chen, Y. Wang, A. Ji, Y. Gao, Novel synthesis of pure VO₂@SiO₂ core@shell nanoparticles to improve the optical and anti-oxidant properties of a VO₂ film, *RSC Adv.* 6 (2016) 108286–108289, <https://doi.org/10.1039/c6ra20636k>.
- [96] Z. Qu, L. Yao, J. Li, J. He, J. Mi, S. Ma, S. Tang, L. Feng, Bifunctional template-induced VO₂@SiO₂ dual-shelled hollow nanosphere-based coatings for smart windows, *ACS Appl. Mater. Interfaces* 11 (2019) 15960–15968, <https://doi.org/10.1021/acsami.8b22113>.
- [97] N.A. Fleer, K.E. Pelcher, J. Zou, K. Nieto, L.D. Douglas, D.G. Sellers, S. Banerjee, Hybrid nanocomposite films comprising dispersed VO₂ nanocrystals: a scalable aqueous-phase route to thermochromic fenestration, *ACS Appl. Mater. Interfaces* 9 (2017) 38887–38900, <https://doi.org/10.1021/acsami.7b09779>.
- [98] Y. Li, S. Ji, Y. Gao, H. Luo, M. Kanehira, Core-shell VO₂@TiO₂ nanorods that combine thermochromic and photocatalytic properties for application as energy-saving smart coatings, *Sci. Rep.* 3 (2013) 1370, <https://doi.org/10.1038/srep01370>.
- [99] Y. Chen, X. Zeng, J. Zhu, R. Li, H. Yao, X. Cao, S. Ji, P. Jin, High performance and enhanced durability of thermochromic films using VO₂@ZnO core-shell nanoparticles, *ACS Appl. Mater. Interfaces* 9 (2017) 27784–27791, <https://doi.org/10.1021/acsami.7b08889>.
- [100] Y. Ke, I. Balin, N. Wang, Q. Lu, A.I. Tok, T.J. White, S. Magdassi, I. Abdulhalim, Y. Long, Two-dimensional SiO₂/VO₂ photonic crystals with statically visible and dynamically infrared modulated for smart window deployment, *ACS Appl. Mater. Interfaces* 8 (2016) 33112–33120, <https://doi.org/10.1021/acsmami.6b12175>.
- [101] L. Zhou, J. Liang, M. Hu, P. Li, X. Song, Y. Zhao, X. Qiang, Enhanced luminous transmittance of thermochromic VO₂ thin film patterned by SiO₂ nanospheres, *Appl. Phys. Lett.* 110 (2017) 193901, <https://doi.org/10.1063/1.4983287>.
- [102] C. Liu, I. Balin, S. Magdassi, I. Abdulhalim, Y. Long, Vanadium dioxide nanogrid films for high transparency smart architectural window applications, *Opt. Express* 23 (2015) A124–A132, <https://doi.org/10.1364/oe.23.00a124>.
- [103] Q. Lu, C. Liu, N. Wang, S. Magdassi, D. Mandler, Y. Long, Periodic micro-patterned VO₂ thermochromic films by mesh printing, *J. Mater. Chem. C* 4 (2016) 8385–8391, <https://doi.org/10.1039/c6tc02694j>.
- [104] Y. Ke, X. Wen, D. Zhao, R. Che, Q. Xiong, Y. Long, Controllable fabrication of two-dimensional patterned VO₂ nanoparticle, nanodome, and nanonet arrays with tunable temperature-dependent localized surface plasmon resonance, *ACS Nano* 11 (2017) 7542–7551, <https://doi.org/10.1021/acsnano.7b02232>.
- [105] Y.-S. Yang, Y. Zhou, F.B.Y. Chiang, Y. Long, Tungsten doped VO₂/microgels hybrid thermochromic material and its smart window application, *RSC Adv.* 7 (2017) 7758–7762, <https://doi.org/10.1039/c6ra24686a>.
- [106] Y. Wang, Z. Fang, J. Wang, A.R. Khan, Y. Shi, Z. Chen, K. Zhang, L. Li, Y. Gao, X. Guo, VO₂/SiO₂/Poly(N-isopropylacrylamide) hybrid nanothermochromic microgels for smart window, *Ind. Eng. Chem. Res.* 57 (2018) 12801–12808, <https://doi.org/10.1021/acs.iecr.8b02692>.
- [107] J. Zhu, A. Huang, H. Ma, Y. Chen, S. Zhang, S. Ji, S. Bao, P. Jin, Hybrid films of VO₂ nanoparticles and a nickel(II)-based ligand exchange thermochromic system: excellent optical performance with a temperature responsive colour change, *New J. Chem.* 41 (2017) 830–835, <https://doi.org/10.1039/c6nj03369e>.
- [108] Y. Zhou, Y. Cai, X. Hu, Y. Long, VO₂/hydrogel hybrid nanothermochromic material with ultra-high solar modulation and luminous transmission, *J. Mater. Chem. A* 3 (2014) 1121–1126, <https://doi.org/10.1039/c4ta05035e>.
- [109] J.T. Zhu, A.B. Huang, H.B. Ma, S.H. Bao, S.D. Ji, P. Jin, Solar-thermochromism of a hybrid film of VO₂ nanoparticles and Coll-Br-TMP complexes, *RSC Adv.* 6 (2016) 67396–67399, <https://doi.org/10.1039/c6ra14232j>.
- [110] J. Zhu, A. Huang, H. Ma, Y. Ma, K. Tong, S. Ji, S. Bao, X. Cao, P. Jin, Composite film of vanadium dioxide nanoparticles and ionic liquid-nickel-chlorine complexes with excellent visible thermochromic performance, *ACS Appl. Mater. Interfaces* 8 (2016) 29742–29748, <https://doi.org/10.1021/acsmami.6b11202>.
- [111] Y. Wang, F. Zhao, J. Wang, L. Li, K. Zhang, Y. Shi, Y. Gao, X. Guo, Tungsten-doped VO₂/starch derivative hybrid nanothermochromic hydrogel for smart window, *Nanomaterials* 9 (2019) 970, <https://doi.org/10.3390/nano9070970>.
- [112] Y. Ke, Q. Zhang, T. Wang, S. Wang, N. Li, G. Lin, X. Liu, Z. Dai, J. Yan, J. Yin, S. Magdassi, D. Zhao, Y. Long, Cephalopod-inspired versatile design based on plasmonic VO₂ nanoparticle for energy-efficient mechano-thermochromic windows, *Nano Energy* 73 (2020) 104785, <https://doi.org/10.1016/j.nanoen.2020.104785>.
- [113] S. Zhao, Y. Tao, Y. Chen, Y. Zhou, R. Li, L. Xie, A. Huang, P. Jin, S. Ji, Room-temperature synthesis of inorganic-organic hybrid coated VO₂ nanoparticles for enhanced durability and flexible temperature-responsive near-infrared modulator application, *ACS Appl. Mater. Interfaces* 11 (2019) 10254–10261, <https://doi.org/10.1021/acsami.8b19881>.
- [114] C. Zhou, D. Li, Y. Tan, Y. Ke, S. Wang, Y. Zhou, G. Liu, S. Wu, J. Peng, A. Li, S. Li, S.H. Chan, S. Magdassi, Y. Long, 3D printed smart windows for adaptive solar modulations, *Adv. Optical Mater.* 8 (2020) 2000013, <https://doi.org/10.1002/adom.202000013>.
- [115] R.S. Zakirullah, Chromogenic materials in smart windows for angular-selective filtering of solar radiation, *Mater. Today Energy* 17 (2020) 100476, <https://doi.org/10.1016/j.mtener.2020.100476>.
- [116] F. Yang, X. Shi, Z. Chen, D. Ma, Y. Wu, H. Luo, Y. Gao, Crystallized TiO₂ (A)–VO₂ (M/R) nanocomposite films with electrochromism–thermochromism dual-response properties, *RSC Adv.* 6 (2016) 32176–32182, <https://doi.org/10.1039/c6ra05700d>.
- [117] T.D. Nguyen, L.P. Yeo, A.J. Ong, W. Zhiwei, D. Mandler, S. Magdassi, A.I.Y. Tok, Electrochromic smart glass coating on functional nano-frameworks for effective building energy conservation, *Mater. Today Energy* 18 (2020) 100496, <https://doi.org/10.1016/j.mtener.2020.100496>.
- [118] S.J. Lee, D.S. Choi, S.H. Kang, W.S. Yang, S. Nahm, S.H. Han, T. Kim, VO₂/WO₃-Based hybrid smart windows with thermochromic and electrochromic properties, *ACS Sustain. Chem. Eng.* 7 (2019) 7111–7117, <https://doi.org/10.1021/acssuschemeng.9b00052>.
- [119] H. Jia, X. Cao, Z. Shao, S. Long, L. Jin, L. Ma, T. Chang, F. Xu, Y. Yang, S. Bao, P. Jin, Dual-response and Li⁺-insertion induced phase transition of VO₂-based smart windows for selective visible and near-infrared light transmittance modulation, *Sol. Energy Mater. Sol. Cells* 200 (2019) 110045, <https://doi.org/10.1016/j.solmat.2019.110045>.
- [120] Y. Gao, S. Wang, L. Kang, Z. Chen, J. Du, X. Liu, H. Luo, M. Kanehira, VO₂–Sb: SnO₂ composite thermochromic smart glass foil, *Energy Environ. Sci.* 5 (2012) 8234–8237, <https://doi.org/10.1039/c2ee21119j>.
- [121] H. Kim, Y. Kim, K.S. Kim, H.Y. Jeong, A.R. Jang, S.H. Han, D.H. Yoon, K.S. Suh, H.S. Shin, T. Kim, W.S. Yang, Flexible thermochromic window based on hybridized VO₂/graphene, *ACS Nano* 7 (2013) 5769–5776, <https://doi.org/10.1021/nr400358x>.

- [122] J. Zheng, S. Bao, P. Jin, TiO₂ (R)/VO₂ (M)/TiO₂ (A) multilayer film as smart window: combination of energy-saving, antifogging and self-cleaning functions, *Nano Energy* 11 (2015) 136–145, <https://doi.org/10.1016/j.nanoen.2014.09.023>.
- [123] H. Ye, L. Long, H. Zhang, B. Xu, Y. Gao, L. Kang, Z. Chen, The demonstration and simulation of the application performance of the vanadium dioxide single glazing, *Sol. Energy Mater. Sol. Cells* 117 (2013) 168–173, <https://doi.org/10.1016/j.solmat.2013.05.061>.
- [124] Z. Chen, Y. Tang, A. Ji, L. Zhang, Y. Gao, Large-scale preparation of durable VO₂ nanocomposite coatings, *ACS Appl. Nano Mater.* 4 (2021) 4048–4054, <https://doi.org/10.1021/acsanm.1c00387>.
- [125] T. Chang, X. Cao, N. Li, S. Long, Y. Zhu, J. Huang, H. Luo, P. Jin, Mitigating deterioration of vanadium dioxide thermochromic films by interfacial encapsulation, *Matter* 1 (2019) 734–744, <https://doi.org/10.1016/j.matt.2019.04.004>.
- [126] T. Chang, X. Cao, L.R. Dedon, S. Long, A. Huang, Z. Shao, N. Li, H. Luo, P. Jin, Optical design and stability study for ultrahigh-performance and long-lived vanadium dioxide-based thermochromic coatings, *Nano Energy* 44 (2018) 256–264, <https://doi.org/10.1016/j.nanoen.2017.11.061>.
- [127] X. Zhou, Y. Meng, T.D. Vu, D. Gu, Y. Jiang, Q. Mu, Y. Li, B. Yao, Z. Dong, Q. Liu, Y. Long, A new strategy of nanocompositing vanadium dioxide with excellent durability, *J. Mater. Chem. A* (2021), <https://doi.org/10.1039/d1ta02525b>.